Title	The Novel Mechanism for Folding of Multicellular Sheets - An Analysis of Inversion of Volvox embryos -
Author(s)	西井, 一郎
Citation	大阪大学, 1999, 博士論文
Version Type	VoR
URL	https://doi.org/10.11501/3155177
rights	
Note	

The Novel Mechanism for
Folding of Multicellular Sheets

– An Analysis of Inversion of *Volvox* embryos –

Ichiro Nishii

A Dissertation Presented to the Department of Biology,
Graduate School of Science, Osaka University
In Fulfillment of the Requirements of the Degree Doctor of Philosophy

1999, January

Acknowledgements

Table of Contents

Abbreveations

BDM	2,3-butandione monoxime
BSA	bovine serum albumin
CTAB	cetyltrimethylammonium bromide
DAPI	4',6-diamidino-2phenynldole
DIC	differentiali nterference contrast
DMSO	dimethylsulfoxide
DTT	dithiothreitol
ECM	extracellular matrix
FITC	fluorescein isothiocyanate
PBS	phosphate buffered saline
PEI	polyethylenimine
RFLP	restriction fragment length polymorphism
SVM	standard Volvox medium

Abstract

Inversion of *Volvox* is an embryonic morphogenetic process in which a series of cell shape changes causes the embryo inside out. This phenomenon has been one of the simplest models to understand the mechanisms of multicellular sheet folding, such as gastrulation, neurulation, and so on. Here it is shown that inversion could be dissected into three cellular processes; (1) changes in cell shape, (2) migration of cytoplasmic bridges, and (3) the global contraction of the pre-inversion portion of the embryo. Previous studies have shown that changes in the individual cell shape are driven by microtubules. I have re-examined the localization changes of microtubules during inversion by fluorescent microscopy and these data support the function of microtubules that determine the cell shape. Next, I have demonstrated that there is an actomyosin-operated contractile mechanism that facilitates passage of the posterior hemisphere through the narrow opening. This is a novel mechanism for inversion. When this contractile force is inhibited with cytochalasins and BDM, inversion is arrested halfway. Third, I observed that migration of the cytoplasmic bridges during bend formation occurred, as in control embryos, even in embryos treated with cytochalasins and BDM. Since the previous observations that the presence of microtubules crossing and running through the bridge. These data collectively suggest that microtubules are responsible for the migration.

To investigate further the mechanisms of inversion, I have isolated transposon-tagged mutants by using less-phototaxis as a marker. In an attempt to correlate genetic identity to the three cellular processes, I have obtained several different phenotypes with distinct defects resulting in the arrest of inversion.

Chpater I
General Introduction

Folding of Multicellular Sheet is a Key for Understanding Morphogenesis

Folding of a multicellular sheet is a widespread embryological phenomenon that is observed during gastrulation, neurulation and various other aspects of morphogenesis in many organisms. Typically, a multicellular sheet is composed of a few types of cells that are tightly linked and arranged in one plane. In the early development, a spherical sheet of blastula is first constructed as an origin, and then it form the organism by the series of folding processes, such as invagination, evagination, and complicated combination of them. Indeed, it is no exaggeration to say that most of multicellular organisms are formed mainly by this process. It is also involved in the various developmental phenomena since it consequently make compartments in organism, such as ectoderm, mesoderm and endoderm by gastrulation, and results in differentiation dependent on each compartment. Thus, this process is a key for understanding morphogenesis.

The folding processes of multicellular sheet have been analyzed extensively at the cellular level, where it has been repeatedly observed that the cells constituting a folding sheet undergo a predictable series of morphological changes in a spatiotemporally regulated fashion (Ettensohn, 1985, Fristrom, 1988). The characteristic wedge-shaped, also called flask- or bottle-shaped, cells have identified in the curvature of the sheet in many cases. Further study, however, has not progressed so far, especially in the molecular level. It is a contrast to some kinds of developmental studies that have progressed to discuss molecules such as HOXs, CAMs, and

cadherins, which are related to pattern formation. While one of goals for molecular biology of pattern formation is finding a certain pattern-corresponding molecule or gene expression, that for multicellular sheet folding seems to be different. Alternatively, we need to know the molecules that cause the dynamic changes of sheet folding. Thus, the force generative molecules, such as cytoskeletal molecules, are intriguing. There have, however, been significantly fewer analyses of the subcellular events that underlie coordinated changes in cell behavior during folding. A simple model system especially for the study of the folding of the multicellular sheet is required because the process in vertebrate is too complex and involves too many features.

Inversion in Volvox as a Simple Model

Inversion of *Volvox* embryo provides a useful model for the study of sheet folding (Kirk et al., 1982). It is a morphogenetic event that occurs in the late embryogenesis of *Volvox* life cycle (Figure 1-1). A *Volvox* embryo is a hollow spherical monolayer of about 3,000 cells. All cells in the embryo, including the 16 larger cells that are destined to become "gonidia", (reproductive cells), are structurally connected by numerous cytoplasmic bridges. There is, however, a region at the anterior pole where the syncytium is interrupted by an opening called the phialopore (Green and Kirk, 1981). As inversion starts, a portion of the sheet encircling the phialopore curls outward to produce a circular bend region. The bend region then moves progressively toward the opposite pole, eventually causing the spherical sheet to turn completely inside out (Figure 1-2 A, Kelland, 1977). *Volvox* inversion bears a certain similarity to metazoan gastrulation, except that it progresses in the opposite direction, and goes to completion. While *Volvox* is green algae, inversion shares many

common features with that of higher animals as the simplified style.

There are at least two advantages of *Volvox* that attract researchers in this field, which seems to be impossible virtually in the other organisms. First, the structure of the multicellular sheet concerned with inversion is very simple. As described above, it consists of only one type of somatic cells. This means no complex cell-cell interaction such as that between epithelia and messenchymal cells, which is stressed in complicated organogenesis. In addition, it has been shown that a common *flask*-shaped cell in inversion (Figure 1-2 B) is generated by individual cell itself. Kelland (1964) first showed in his doctoral thesis that mechanically isolated cells deformed their shape as they had been in an intact embryo. Viamontes and Kirk (1977) confirmed this and they have also observed the migration of cytoplasmic bridges in a cluster of three cells. It may sound natural tha the *flask*-shaped cell formed by itself but such a direct demonstration is not so easy since it is a rare case that an isolated cell maintains its deformability as in whole embryo. For example, the 'purse-string' hypothesis, which proposes that circumferential bands of actin microfilaments at the apical side of epithelial cells constrict to yield a curved epithelial sheet, has been widely believed to explain invaginations during embryogenesis. However, the direct demonstration at an isolated cell level has never observed yet. In fact, there's other possibilities that the cell surrounding the *flask*-shaped cell could generate force to induce it flask-shaped and/or that other than cell such as extracellular matrix could be involved (Lane et al., 1993). In *Volvox* the cell sheet is a monolayer without a basal membrane that lines the epithelia with ECM-rich material. ECM is not secreted until the stage of inversion while adult cells are embedded with it. Thus, we can focus the behavior of only one cell type during inversion. It does not mean I intend to deny the involvement of

extracellular interaction in inversion. In fact, it has been shown that antibodies against a certain kind of glycosphingo-lipid and Algal-CAM had an inhibitory effect on inversion (Huber and Sumper, 1994, Wenzl and Sumper, 1986). These studies implied the extraellular interactions have been involved in inversion although their roles were still unknown. Despite of it, the situation must be much simpler than the other animals.

Second, it has been shown that several types of morphological mutants, including inversion-deficient ones, are available in *Volvox*. It is a rare case that mutants that fail the folding of the multicellular sheet, such as gastrulation, are obtained because this process is ubiquitous and essential in development and thus such mutants are considered to be lethal. In contrast, inversion is not essential for viability of *Volvox*. The germ line, the larger cells that are embedded in somatic cell layer (Figure 1-2 B), is differentiated before inversion and become mature in the inversion-less

mutants. Moreover, differently from other animals, the autotrophism of this organism enable mutants to grow even in such abnormal morphology by which the animals may have a trouble in predation. Molecular analysis of the mutants for the folding of the multicellular sheet seems to be only possible in *Volvox* inversion and thus unique information could be anticipated if such analysis would be possible.

Cytoskeletal Proteins are Involved in Cell Shape Changes during Inversion

The behavior of somatic cells in inversion is previously described in detail (Kelland, 1977, Viamontes and Kirk, 1977). The cell shape dynamically changes during inversion. In the bend region, the unique *flask*-shaped cells are seen as in the case of the folding of the multicellular sheet in vertebrate (Figure 1-2 B). Cytoskeletal proteins are shown to be involved in such cell shape changes. Microtubules that underlie

- 5 -

beneath the plasma membrane elongate in concert with cell elongation and the polymerization of tubulin is shown to be essential for inverison (Viamontes et al., 1979). Although another cytoskeleton, actin filaments, has been considered to be involved in inversion, especially in the process of the migration of the cytoplasmic bridges (Viamontes et al., 1979), the information about their localization have been completely lacked so far and thus the role of actin filaments in inversion seems to be obscure.

In the second chapter in this thesis, I examine the role of actin filaments and myosin molecules in inversion to elucidate further the mechanism of force generation in inversion at the molecular level. In addition to their localizations, I have investigated the function of them by using several inhibitors and microsurgery of embryos. The ultra-structual data have shown that the migration of the cytoplasmic bridges is not dependent on actin, which was proposed previously (Viamontes et al.,

1979, Green et al., 1981). Moreover, actin and myosin are not essential for the cell shape changes in the bending region (Figure 1-2). Instead, they work in the different region where the bend have not reached. Actin filaments and myosin contracts the pre-inverted region, which is essential for the smooth propagation of the bend from the phialopore to the opposite pole. It is noteworthy that two of the previosuly isolated mutants, called 'Tulip' and 'Jester's cap' (Kirk et al., 1982), showed the phenotype that resemled the arrested inversion with actomyosin inhibitors. Combined with the previous data, I finally propose how the cytoskeletal proteins work in inversion.

The Molecular Biological Analysisof Mutants Become Possible in Volvox carteri

The relationship between the pheno-type of the mutants and the affected inversion with actomyosin inhibitors spontaneously direct me to the analysis

of the mutants. It seems to be enough interesting if I would examine the mutants with microscopy and micros- urgery to compare with the results for the embryos treated with the inhibitors by obtaining them from other reseachers who have been keeping them. I noticed, however, that this methodology will meet soon the limitation since those instantly available mutants are only mutants; they give me no genetic information. In *Volvox* we have no means to clone the gene from previsouly isolated mutants with chemical or UV mutagenesis, such limitation is common in almost all eucaryotic organisms except for *Arabidopsis thaliana*, *Chlamydomonas reinhardtii*, *Dictyo- stelium discoidium* and so on.

Fortunately, the two latest papers could finally overcome this limitation in *Volvox* (Kirk et al., 1999, Miller and Kirk, 1999). Kirk and his colleagues have first isolated a transposon that showed heat- or cold-inducible trans- position (Miller et al., 1993). They have utilized the insertion of this transposon as a tag and have isolated the novel genes that is essential for germ-soma differentiation of *Volvox*. In the third chapter, I attempt to re-isolate the mutants deficeint in inversion with this newly developed method.

Apparently, the barrier for selection of the mutants is how to screen the inversion-less ones. Though the frequency of *Jordan* transposition increases by heat- or cold-shock, it is not comparable with that by the chemical mutagenesis. To innovate efficient screening method seems to be critical for this study. Althoug inversion itself is not directly utilized as a marker for screening, I noticed it is well linked to physiological properties of *Volvox*. It is easy imagine that an inversion-failed spheroid will not be a good swimmer. The abnormal morphology must affect the style of swimming. Thus, the phototaxis, which is a common feature of green organisms, have a potential for the screening method and how it

successfully works for the screening is described in the third chapter.
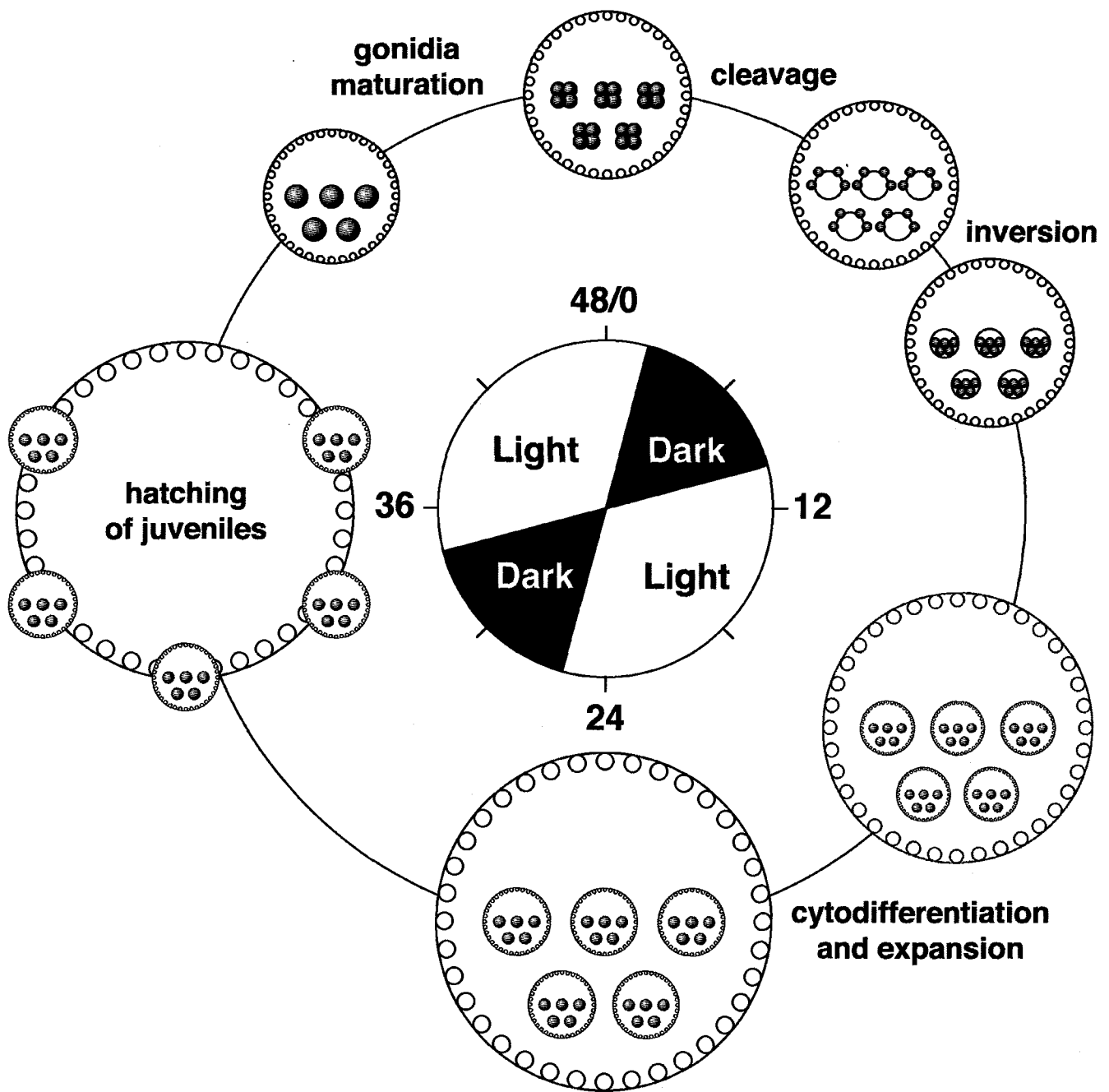
Figure 1-1. Life cycle of *Volvox carteri*.

By the light-dark cycle shown in the center, the life cycle of *Volvox carteri* can be synchronized. Near the end of the light period, the gonidia begin a rapid series of cleavage. It was finished in the early dark period. Next, inversion is occurred and the embryos assume the adult conformation in which the newly generated premature gonidia are placed inside. In the next light period, they become expanded with secretion of ECM. In the next light period, the juveniles digest their parent and become adults. Meanwhile the gonidia become maturated and initiate a new round of embryogenesis. This picture was based on the Figure of the book 'Volvox' p.125 written by David L. Kirk and I modified the light cycle as used in this thesis.

A
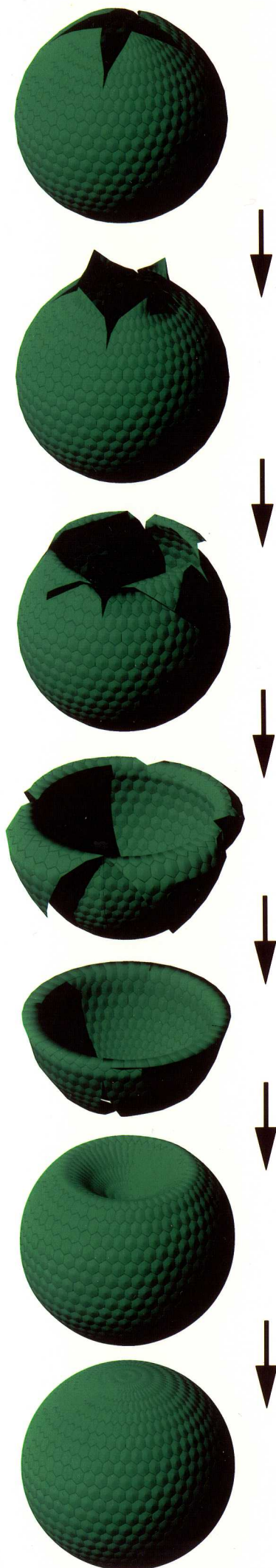
B
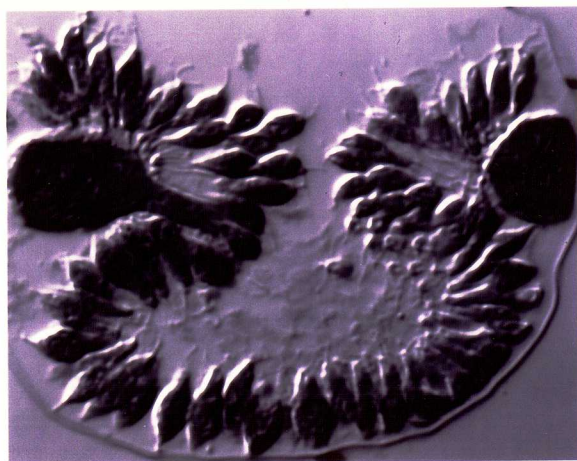
C
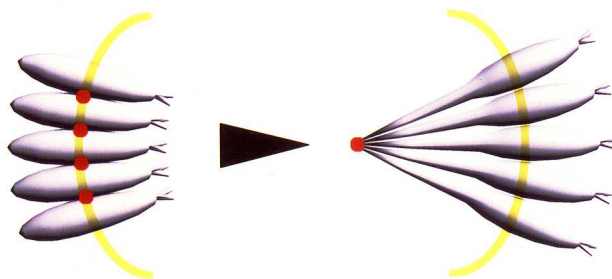
Figure 1-2. Inversion of *Volvox*.

(A) The sequential changes of embryonic morphology during inversion are illustrated by 3D graphics. The phialopore first opens and then the four lips of the phialopore, the cross slits in the anterior, turn outward. The bending movement progressively propagates toward the posterior pole and results in the embryo inside out. The whole inversion takes about 45 minutes. (B) The section of mid-inversion embryo is shown. The small somatic cells are aligned as a monolayer and two large gonidia are embedded in. (C) The transformation from *spindle*, which are located in the pre-inverted region in (B), to *flask*-shaped cells, which are located in the inverted region in (B), are illustrated. The red dots show the location of the cytoplasm bridges that link cells. They are migrated in parallel to the *spindle* to *flask* transformation.

Chapter II
Role of Actomyosin Contraction of
Inversion of *Volvox Carteri* Embryo

Introduction

As described in the chapter I, during bend formation in inversion of *Volvox carteri* embryo, two cellular events, i.e., specific shape changes and movements of the cytoplasmic bridges, have been reported to take place (Kelland, 1977; Viamontes and Kirk, 1977; Viamontes et. al., 1979; Green et al., 1981). Just prior to inversion the cells become *spindle*-shaped from *pear*-shaped and they are linked by cytoplasmic bridges at their widest points at their nuclear level. Cells in the bend form long, narrow projections at their outer ends (becoming *flask*-shaped), and simultaneously the cytoplasmic bridges move so that they become bundled at the tips of these projections (the chloroplast end; which faces to outside before inversion and become inside of the curvature when inverted). The bend is then propagated progressively from the phialopore toward the opposite pole by movement of a circular zone where these two cellular events are taking place (Viamontes and Kirk, 1977). Propagation of the bend obviously requires precise spatiotemporal regulation of cell shape and movement (Green et al., 1981).

Kirk and his colleagues have implicated microtubules and actin filaments in the two cellular events of inversion (Viamontes et al., 1979). Microtubules were implicated by two observations; first, an ultrastructural analysis revealed abundant microtubules aligned along the thin stalks of flask cells (Viamontes and Kirk, 1977). Second, colchicine or low temperature treatments as the depolymerizing factor of microtubules, which inhibited inversion, abolished elongated cells,

otherwise present in the bend (Viamontes et al., 1979). Inversion was also blocked by inhibitors of actin filaments (Viamontes et al., 1979). In contrast, Ireland and Hawkins (1980) have reported that inversion of a different species, *Volvox tertius*, was not inhibited with cytochalasin B. In addition to such an inconsistent data, actin filaments were not examined for its cellular locations. Thus the cytological basis for the cytochalasin effect was not fully explained and it needs further investigation in detail.

In this study I analyze the spatial distributions of actin filaments, myosin, microtubules and other structures in an inverting embryo by fluorescence and electron microscopy. Combining such studies with the use of actomyosin inhibitors and microsurgery, I provide evidence that localized actomyosin contraction, which is generated so as to make the posterior hemisphere compact, appears to be essential for inversion.

This constitutes a previously unrecognized aspect of the inversion process.

Materials and Methods

Culture and Preparations of Embryos for Experiments

Volvox carteri f. nagariensis, strain HK-10 was obtained from the University of Texas Culture Collection of Algae. The axenic culture was maintained in a synchronous and asexual growth with the standard Volvox medium (SVM: 0.5 mM $Ca(NO_3)_2$, 0.16 mM $MgSO_4$, 0.67 mM KCl, 0.19 mM Na_2CO_3, 2.1 μM $FeCl_3$, 1.2 μM $MnCl_2$, 0.22 μM $ZnCl_2$, 0.05 μM $CoCl_2$, 0.1 μM Na_2MoO_4, 0.23 mM sodium glycerophosphate, 0.5 mM urea, 13.4 μM disodium ethylenediamine tetraacetic acid, 3.0 μM thiamine, 1.0 nM biotin, 0.1 nM vitamin B_{12}, and 3.8 mM glycylglycine; pH 8.0 adjusted with NaOH ,Kirk and Kirk, 1983) at 32°C under the light cycle conditions previously reported (16 hrs light and 8 hrs dark; Tam and Kirk, 1991). At this light cycle, embryos started inversion at 3-5 hrs later from the onset of the dark period. Volvox spheroids 2-4 days after inoculation were harvested by filtration using a nylon cloth with a 90 μm mesh size (Falcon Cell Strainer: Nippon Bection Dickison Co. Ltd., Tokyo, Japan). They were then ruptured in SVM by five passages from a 1 ml syringe through a 25-gauge needle. The embryos thus released were retrieved on a 40 μm mesh screen after having been passed through a 90 μm mesh screen to remove spheroid debris. Embryos were then rinsed in a large excess of SVM. All experiments thereafter were done at room temperature.

Drug Treatment

Stock solutions of cytochalasin B, D, and E (Sigma Chemical Co., St. Louis, MO, USA) were prepared following the method described previously (Viamontes et al., 1979). They were all dissolved at 10 mg/ml in DMSO (Infinity Pure, Wako Chemicals, Osaka, Japan) and diluted 100-fold in SVM just before use. A myosin II inhibitor, 2, 3-butandione monoxime (BDM; Sigma) was diluted to 40 mM with SVM from a freshly prepared 0.5 M solution (Cramer and Mitchison, 1995). Sucrose at 50 mM was present in all drug solutions to avoid non-specific osmotic damages (Viamontes et al., 1979). The concentration of sucrose was lowered to 10 mM in the case of BDM to balance the osmolarity. I also confirmed that BDM effect was similarly observed even it contained 50 mM sucrose. It seemed that the osomolarity mechanism was not needed in this inhibitory effect on inversion.

To treat embryos with the drugs, isolated embryos were placed on a glass coverslip that were pre-coated with 0.01% polyethyleneimine (Kirk et al., 1993). Prior to drug application, embryos on a coverslip were incubated in 50 mM sucrose in SVM for about 60 minutes. An appropriate amount of the drug solution was

placed onto the embryos and the solution was changed quickly two more times to facilitate solution exchange. Removal of drugs was done similarly with 50 mM sucrose in SVM without a drug.

Video Microscopy

Embryos prepared by the method described above were not completely synchronous but varied by about 2 hour in developmental stage, and thus individual embryos initiated inversion over a period of 2 hours. For this reason, I employed video microscopy for continuous monitoring of live embryos, which enabled me to treat individual embryos at any specific stage of inversion.

Embryos were observed by differential interference contrast (DIC) on an Olympus inverted microscope (IMT-2, Olympus, Tokyo, Japan) with LWD CDPlan40PL/0.55, LWD CDPlan20PL/0.40 and SPlan4PL/0.13 and the images were recorded with a cooled CCD video camera (Image Point; Photometrics, Ltd., Tucson, AZ, USA) onto S-VHS video tapes by a VCR (HV-BS53; Mitsubishi, Tokyo, Japan). Images were occasionally enhanced with an image-processor, S-III (Nippon Avionics Co., Tokyo, Japan) and captured on a Macintosh 840AV (Apple Computer, Cupertino, CA, USA) with software NIH Image 1.59. Edited digital images were printed with a color printer

(Pictrography 3000: Fujifilm, Tokyo, Japan). For higher resolution, images were recorded with a high resolution cooled CCD camera (PXL-1400; Photometrics) mounted on a Nikon Optiphoto II with Plan40/0.70 DIC and Ph1DL10/0.25 (Nikon, Tokyo, Japan) or on a Olympus AX-70 with UplanApo 10x/0.40, UplanApo 20x/0.70 and UplanApo 40x/0.85.

Sectioning Plastic Mounted Specimens for Optical Microscopy

To acquire images with single-cell resolution, embryos were processed as follows. While recording with videomicroscopy to track each, embryos isolated as above method on a coverslip were fixed in 2% formaldehyde, 2.5% glutaraldehyde, 2.5% tannic acid in 0.02 M phosphate buffer at pH 8.0 for 12-16 hours and post-fixed in 1% OsO_4 in the same buffer for 3 hours (Viamontes and Kirk, 1977). Specimens were then dehydrated in a graded series of ethanol solutions, and infused with Technovit 8100 (Kulzer, Wehrhein, Germany). To capture embryos in a Technovit block mountable on a microtome, a fresh Technovit solution contained in a gelatin capsule was placed upside-down on the coverslip and allowed to polymerize in vacuum for 1 hour. To prevent leakage of the unpolymerized Technovit from the capsule, a silicon rubber o-ring that fit the outer diameter of the gelatin capsule was first placed on the coverslip to surround the embryo samples. After

polymerization, 2.5 μm-thick serial sections were cut with a glass knife on an ultramicrotome (Reichert Ultracut E: Leica, Vienna, Austria). Sections were mounted on glass coverslips with Entellan (Merck, Darmstadt, Germany) and observed with a Nikon Optiphoto II (Plan100/1.25 oil DIC, Plan40/0.70 DIC and Ph1DL10/0.25) equipped with DIC optics. Low magnified images of one section in the entire area were captured with CCD camera, transferred to Macintosh computer and then reconstructed as whole image by using Photoshop 'Layer' function. It was compared with video images that had been recorded before fixation to track each embryo, and thus the time course of inversion of each embryo could be precisely determined as indicated in the legend of Figure 2-9.

Actin filament staining for *Volvox carteri*

Isolated embryos were attached to PEI-coated coverslips and fixed for 15 minutes in 3.7% formaldehyde, 1 mM DTT, 0.1% Triton X-100, 2 mM MgCl2, 5 mM EGTA, 150 mM KCl, 10 mM sodium glycerophosphate, and 10 mM HEPES at pH 7.1, a solution modified from a fixative originally designed for preservation of labile actin filaments of leukocytes (Redmond and Zigmond, 1993). The coverslips were then washed (with gentle agitation) in a Coplin jar containing 1% NP-40, 1 mM DTT, 1% BSA, 2 mM MgCl2, 5 mM EGTA, 150 mM KCl, and 10

mM sodium glycerophosphate for 1 hour to extract chlorophyll and minimize auto-fluorescence. After washing three times in TPBS (0.1% Tween 20) supplemented with 0.1% BSA, embryos were stained for 4 hours with 4 μM fluorescein-phalloidin (Molecular Probes, Inc., Eugene, U.S.A.) in the same buffer, and again washed three times in TPBS. Samples were mounted in 50% glycerol, 1 mg/ml phenylenediamine (an anti-fading agent) in PBS. It is noted that this method well managed both the preservation of actin filaments of *Volvox* and decreasing the autofluorescence. Although alternative method for extraction of auto-fluorescence was using organic solvent such methanol and ethanol at various concentration was attempted, it resulted in the disappearance of all actin filaments. A conventional method for staining of actin filaments without NP-40 extraction was also tried but too strong autofluorescence interfered with the emission of any fluorescent wavelength and it could not be avoided by selecting a certain appropriate fluorophore.

Immunofluorescent staining

For immunostaining, embryos were similarly fixed and incubated for 12 hours either with 10-20 μg/ml anti-tubulin monoclonal antibody (Amersham, Buckingamshire, England), or 10 μg/ml affinity-purified antibodies against Physarum myosin II (Ogihara et al., 1983).

- 15 -

Samples were then washed and stained with an FITC-conjugated secondary antibody (Amersham) at 1:200 dilution for 4 hours. To visualize the nucleus, DAPI (4 μg/ml) was included in the secondary antibody solution. The secondary antibodies were pre-absorbed following the protocol described by Harlow and Lane (1988). The anti-myosin II from *Physarum plasmodium* used in this study was affinity purified and is mono-specific for the heavy chain. Staining without the primary antibody as a control gives no specific patterns (data not shown). It was also observed that the antibody against from *Dictyostelium discoideum* myosin II also gave the same staining pattern (data not shown).

Fluorescent Microscopy

Embryos were imaged on a Photometrics cooled CCD camera (PXL 1400) attached to a Nikon Optiphoto II with Fluor40/0.85 and Plan100/1.25 oil DIC. Serial images in the z-axis were precisely incorporated by the use of a computer-assisted focusing devise (Micro Z-mover; Photometrics). Digitally deconvoluted images were obtained using IPLab and Confocal extension (Signal Analytics Corporation, Vienna, VA, USA), following the method by Agard et al. (1989). Typically, three images with 0.2 μm intervals in z-axis were captured with 100x or 40x objective lens. Before confocal calculation, images were corrected by the background

subtraction by using dark current noise and signal standard by using flat signal. The fluorescent images captured by using different filters were combined with Photoshop by using different 'Channel' to build a pseudo-color image.

Electron Microscopy

Specimens were prepared for electron microscopy as described by Viamontes et al. (1979). Embryos, either drug-treated or untreated, were fixed at 20°C for 15 seconds in 2 ml of freshly prepared 2.5% glutaraldehyde in SVM (pH 7.2), and then 0.5 ml of 2% OsO_4 in H_2O was added. Fixation was continued in the resulting mixture for 10-15 minutes. After washing with SVM, the specimens were transferred to 2.5% tannic acid in H_2O for 15 minutes, washed again in SVM and postfixed in 2% OsO_4 in H_2O for 15 minutes. After another SVM wash, specimens were transferred to 2.5% uranyl acetate in H_2O for 15 minutes, washed in H_2O, dehydrated, embedded and sectioned. The images were taken with Fuji electron-microscopic film (8.2 x 11.8 cm) and scanned with DT-S1015 AIS (Dainippon Screen Mfg. Co. Ltd., Kyoto), Macintosh 8600/200, and the plug-in driver for Adobe Photoshop. To obtain large images with high-resolution, high-magnifed images of small area were combined and then the larger images that covered the whole embryo or

whole one cell was reconstructed as in Figure 2-10.

Microsurgery

Kelland have reported unique experiments by using a microsugery technique that was applied to *Volvox carteri* and *Volvox aureus* (1977). In this experiment, he has used watch maker forceps to tear off "gonidial vesicle" surrounding an inverting embryo and then cut the naked embryo. He, however, described fewer example for *Volvox carteri* than that for *Volvox aureus* since he had difficulty especially for the microsurgery of the former species. When I first attempted to tear off the vesicle by forceps, it appeared to be impossible for me since the embryo was too small with diameter less than 100 μm. To handle more precisely, I decided to use the micromanipulator and the tungsten needle with a fine tip that was sharpend by electrolysis. By using this sysytem, I could make a tiny opening in the vesicle, unfortunately it resulted in fault. As soon as the small opening was made on veiscle, the embryo inside spontaneously go outside through the opening and cells became dissociated from each other when they passed. If I had made tearing off the vesicle instantly, such an undesired result would be avoided. The vesicle, however, was too tough to cut at a stroke. Although several enzymes such as cellulases and glycosidases were tested for

digestion of the vesicle, they did not affected at all.

The alternative method that was described by Ransick (1991) was first applied to *Volvox obversus*. He treated the embryo at the one- or two-cell stage with trypsin to soften the vesicle and then could tear it off easily with forceps. Moreover, he also applied this method successfully to *Volvox carteri* (Kirk et al., 1993). I followed Ransick's method with modifications as follows. Gonidia (the asexual reproductive cells from which *Volvox* embryos are derived) were isolated by the method described above for embryos and then were incubated in SVM containing 0.1 mg/ml trypsin (Type XIII, Sigma) for 15-30 seconds and washed with an excess volume of SVM containing 1% BSA. The specifc type of trypsin was critical for this effect. The softened vesicles were then removed from the embryos with micromanipulation using a fine tungsten needle sharpend with electrolysis. After the trypsin treatment, the space become to be found between vesicle and gonidia in 5-10 minutes. If too short, the gonidia was too fragile to keep its morphology when pressed with a needle, resulting in puncture and death. At first, the needle was slowly placed over the gap , and it was tightly pressed to the coverslip. At that time, only the vesicle were sandwiched between the needle and coversplip. When the needle was quickly pressed and pulled, the substantially long

slit was made in the vesilce and the gonidia could be isoalted from the veiscle through the slit. Vesicle-free embryos were transferred to SVM contained in a plastic ELISA plate and allowed to develop for about 8 hours. After the final cleavage, vesicle-free embryos were transferred to a ~200 μl drop of SVM placed on a silicon-coated coverslip. Non-siliconized coverslips or normally used PEI-coated ones were adhered to cells too much and destroyed the embryo. Most of the anterior half was then removed from the embryo by pressing a fine glass needle along the equatorial plane.

Morphometry

To measure the width of the posterior hemisphere of inverting embryos with high geometrical accuracy, the digitized images were rotated so that the antero-posterior axis became the y-axis of the analysis coordinate. The posterior hemisphere diameter was then obtained as the maximal surface-to-surface dimension parallel to the x-axis. Quantification and calculation were done using NIH Image 1.59 and Igor Pro 3.02 (Wave Metrics, USA).

Results

Microtubules Rearrangements Accompany Cell Shape Changes that Occur during Inversion

Cells changed shape conspicuously during inversion, as seen in the DIC images (Figure 2-1). The sequential change of the cell shape are consistent with the previous report by Viamontes et al. (1979), who named the characteristic shapes *pear*, *spindle*, *flask* and *column* according to the progression of inversion. The *pear*-shaped cells at the pre-inversion stage (Figure 2-1 A, F) were nearly round with slightly conical anterior ends, the apices of which were directed toward the interior of the embryo. The nucleus was also conical, with its apex aligned with that of the cell. The phialopore opened, as cells assumed an elongated *spindle*-shape with a short protuberance pointing outward (Figure 2-1 B, F). In the characteristic bend region near the phialopore, there were *flask*-shaped cells

with the long stalks (Figure 2-1 C, F). Cells remained elongated throughout inversion (Figure 2-1 C, D, F), but then assumed a less-elongate *column*-shape again after inversion had been completed (Figure 2-1 E, F). Concomitant with these cell shape changes, the distribution of microtubules changed dynamically. In pre-inversion embryos, the microtubule signal outlined each cell in fairly uniform manner (Figure 2-1 A, F), but once cells became elongated they exhibited an much more intense microtubule signal in regions distal to the nuclei, at the chloroplast outer ends of the cells (Figure 2-1 B, C, F). Although individual microtubules were not resolved highly, the microtubules appeared to be aligned parallel to the long axis of each cell. Nuclei were located close to the inner surface in uninverted portions of the embryo. Flagella became visible on the newly exposed outer surface, in close proximity to the nucleus, in embryos approaching the end of inversion, (Figure 2-1 D, E,
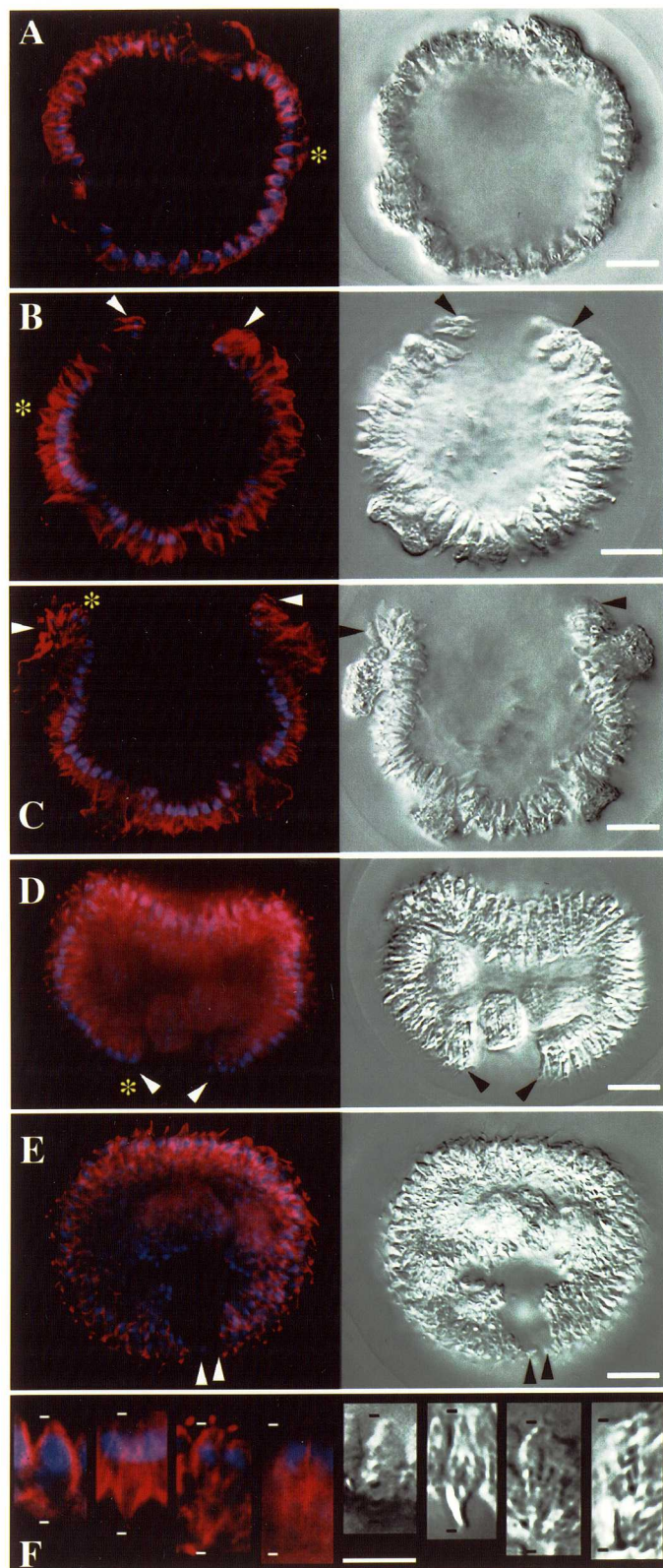
Figure 2-1. Localization of microtubules in *Volvox carteri* embryos during inversion.

Localization of microtubules in Volvox *carteri* embryos during (A) the pre-inversion stage, (B) phialopore opening, (C) early inversion, (D) late inversion, and (E) the post-inversion stage. In F, 4 pairs of magnified images of the cells characteristic to embryos in the specific stages of inversion are shown; 'pear', 'spindle', 'flask', and 'column'-shaped cell (Viamontes *et al.*, 1979), from left to right. The approximate locations of the corresponding cells in the low magnification images are indicated with asterisks in A-D. The left image in each pair shows the location of tubulin (red) and the nucleus (blue), and the right one shows the same embryo by DIC. Cells changed shape conspicuously during inversion (F). Microtubules outlined the cell shape initially in the pear-shaped cells (A), and then became much more abundant in the posterior (outer) ends as the cells elongated in the spindle-and flask-shaped cells (B, C). Enhanced tubulin signals on the nuclear ends of the cells (D, E) reflects the beginning of the flagellar elongation following inversion in the columnar cells. Arrowheads in A-D indicate the opening of the phialopore. Bar; 10 μm (A-E), and 5 μm (F).

F). These data well support the idea by Viamontes et al. (1979) based on the ultrastructual study that microtubules are involved in the series of cell shape changes during inversion.

Actin Filaments Also Undergo Dynamic Changes during Inversion

I next examined the cellular localization of actin filaments by use of fluorescein-phalloidin. Since the actin filaments of *Volvox* were labile I needed to develop the appropriate stainning method. The staining method shown in Figure 2-2 well stained actin filaments of *Volvox*. It is noted that the auto-fluorescence were also decreased, too. Since chloroplasts and plastids that occupied almost half area of cells had strong autofluorescence, it was impor-tant to obtain fluorescent signals without their interference. As shown in Figure 2-2, when non-fluorescent-phalloidin was added in varying proportions to the fluorescein-phalloidin staining solution, it caused a substantial, concentration-dependent decrease in the fluorescent signal. This led me to conclude that the fluorescent signal obtained with fluorescein-phalloidin is phalloidin-specific, and hence, presumably actin-specific.

Actin filaments were dynamically changed their localization pattern during inversion in different way from that of microtubules. In pre-inversion embryos most actin filaments were restricted to the perinuclear cytoplasm in *pear-shaped* cells; none were detected in the chloroplast region (Figure 2-3 A, E). As inversion began, a dramatic change in the organization of actin filaments occurred; the intense perinuclear signals were replaced by a more-or-less continuous, subnuclear actin filament array that traversed the entire embryo from one pole to the other (Figure 2-3 B, F). Indeed, this filament array appeared to be continuous through the cyto-plasmic bridges known to be linking adjacent cells at this stage (Figure 2-3 G). This shift in actin-filament location
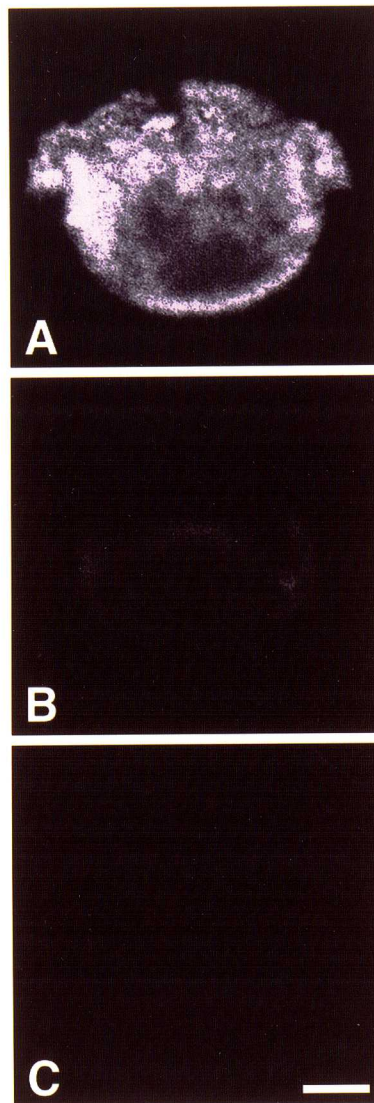
Figure 2-2. Actin filaments of *Volvox carteri* are specifically stained with fluorescein-phalloidin.

The specificity of the phalloidin staining was demonstrated. Embryos were stained with fluorescein-labeled phalloidin only (A), an equimolar mixture of labeled and unlabeled phalloidin (B), and a 10-fold excess of unlabeled phalloidin (C). Unlabeled phalloidin inhibited the fluorescein signals competitively and thus the signals are shown to be phalloidin specific. It is noted that autofluorescence are perfectly decreased in this staining method (C). This is a first report of staining of actin filaments in *Volvox* so far.

Figure 2-3. Localization of actin filaments are dynamically changes during inversion.

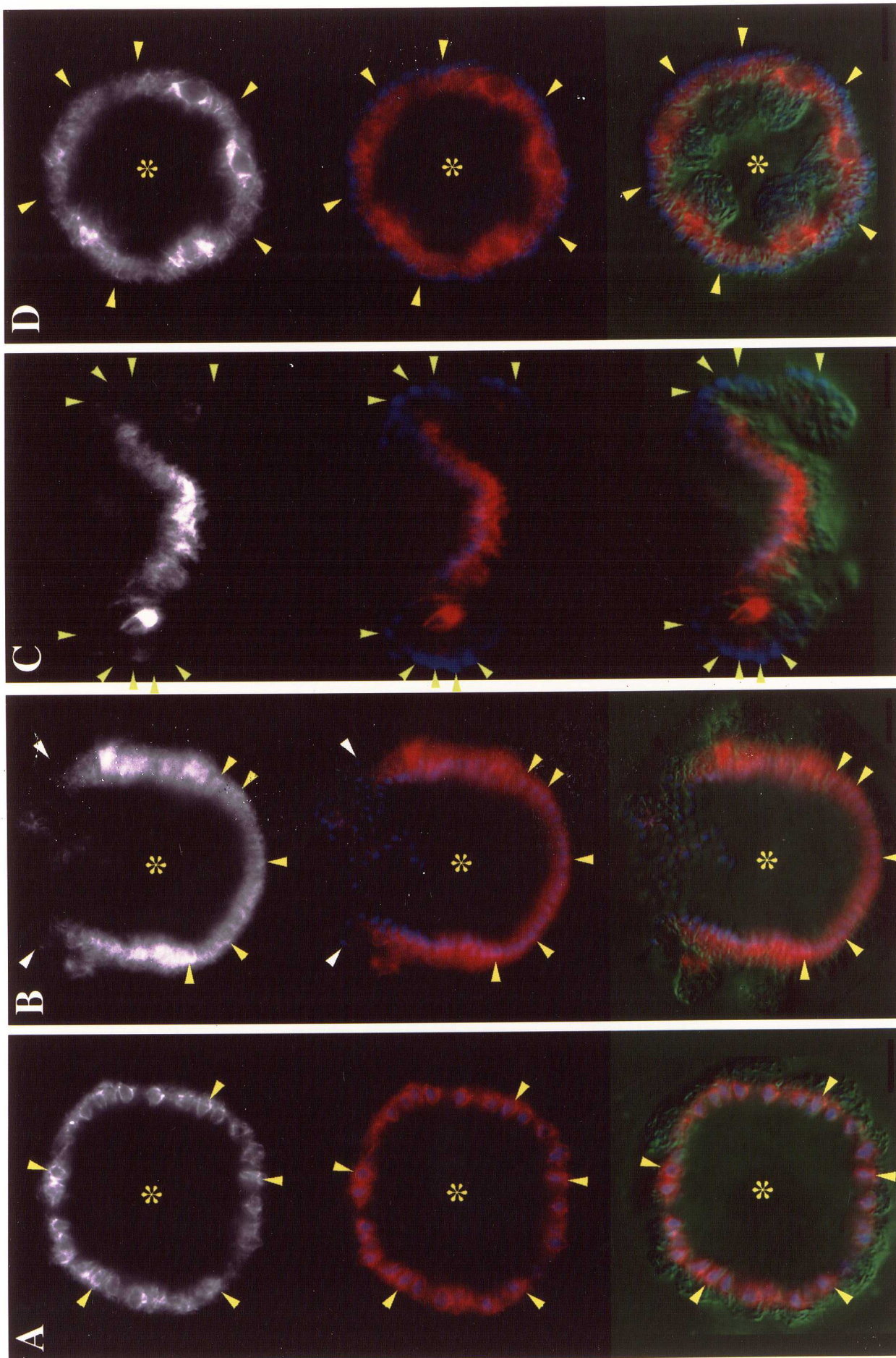Each inversion stage (A-H) is represented by a set of images, in which the top one shows only the localization of actin, the second one adds the location of the nucleus (blue) to actin (red) and the bottom one adds the DIC image (green). Arrowheads are placed to indicate the outer ends of the nucleus so that the cellular locations of actin filaments relative to the nucleus and the chloroplasts may be recognized easily among the sets of images. Asterisks indicate the embryo coeloms in any cases. At the pre-inversion stage (A,E), actin filaments
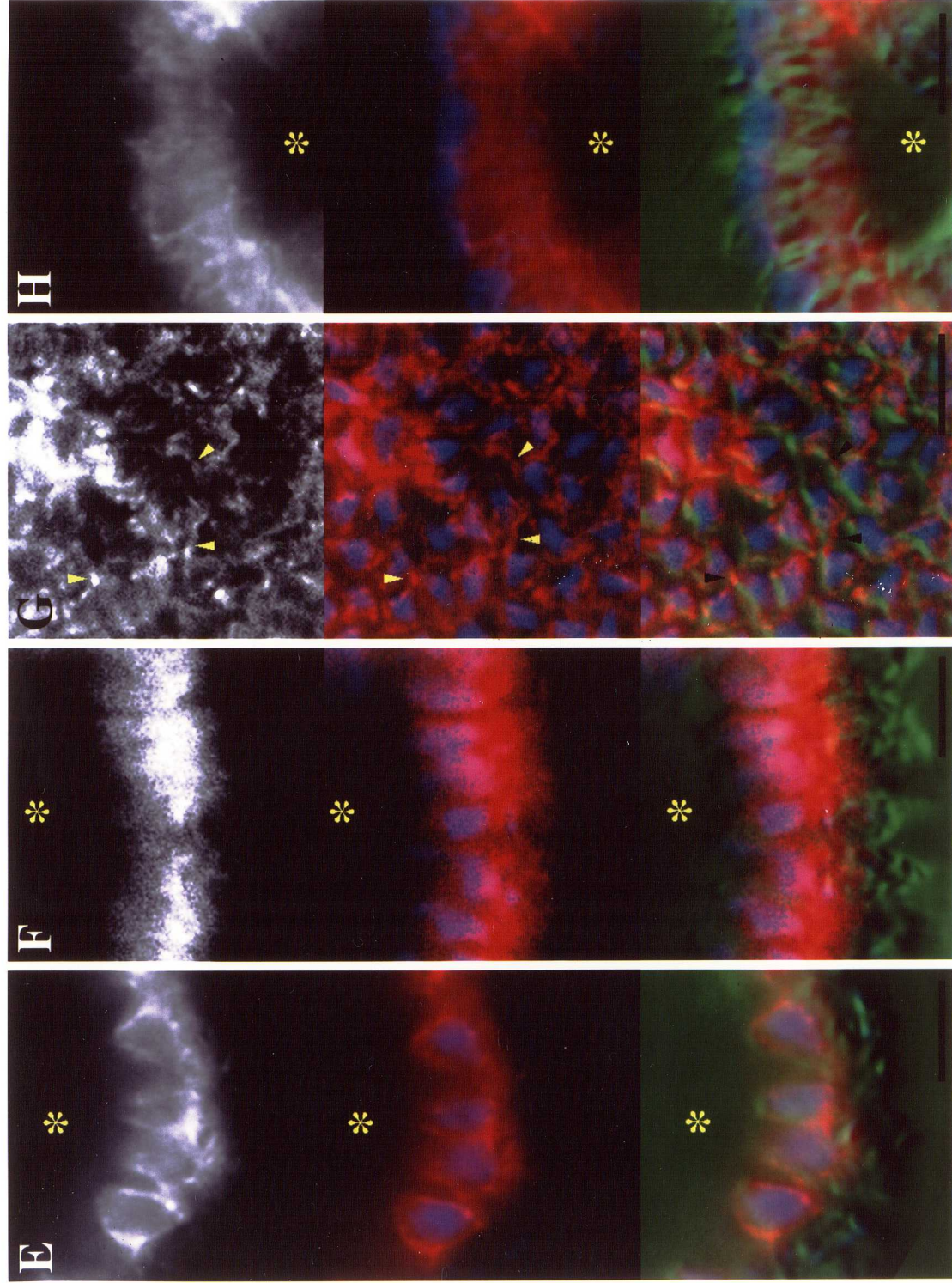
were localized in the perinuclear region and absent in the chloroplast region (arrowheads). As the phialopore opens (black and white arrowheads) actin filaments moved toward the chloroplast (outer) ends of cells throughout the embryo (B, yellow arrowheads; F). As inversion proceeds actin filaments disappeared from cells entering the bend region and remained absent until inversion had completed. Then, once inversion had completed, the diffuse actin filament signal returned to the chloroplast (now inner) ends (*) of all cells (D, arrowheads; H). As evident in the magnified images, the perinuclear signal (E) moved to regions between the nucleus and the chloroplast (F) to form the characteristic continuous belt-like zone. This intense signal was found not only in the bodies of the cells but also in the bridge-like structures linking adjacent cells (arrowheads in G). Bar; 10 μm (A-E, and J) and 5 μm (F-I).

appears to be much more extreme in the anterior (phialopore-proximal) hemisphere than in the posterior hemisphere at the beginning stage of inversion (Figure 2-3 B). As inversion proceeded (Figure 2-3 C), the actin filaments were displaced somewhat toward the chloroplast ends of the *spindle*-shaped cells of the uninverted cells, where they formed an intensely staining band that was continuous throughout the posterior portion of the embryo. In marked contrast, actin filaments virtually disappeared from cells that had entered or passed through the bend region of the embryo where *flask*-shaped cells were observed (Figure 2-3 C, arrowheads). After inversion was complete, diffuse actin signals returned to somatic cells (Figure 2-3 D), and more intense signals were observed in the gonidial cells.

Because the images obtained with whole embryos made it appear that the actin array in the uninverted portions of an embryo was continuous from cell to cell (Figure 2-3 C, F),I next examined

optically sectioned embryos from a different angle, in an attempt to obtain higher resolution and to determine if this actually was the case. Figure 2-3 G shows a cross-section of the posterior hemisphere of an inverting embryo in which some cells appear to have protrusions linking them to adjacent cells (which presumably is a reflection of the cytoplasmic bridge system known to link cells at this level at this time; Green et al., 1981). Actin staining is present in such protrusions.

Myosin II is Co-localized with Actin Filaments in the Uninverted Portion of the Embryo

Antibodies against myosin II of Physarum plasmodia (Ogihara et al., 1983) cross-reacted with *Volvox* myosin. Before inversion, myosin II was localized in the perinuclear region in a pattern similar to that of the actin filaments (Figure 2-4 A, D). In addition, a discrete spot of intense myosin staining was observed at the inner end of *pear-*

shaped cell, in a region known to be occupied by the basal bodies and contractile vacuoles.

During inversion, myosin II, like actin, became localized to a subnuclear cytoplasmic region in a *spindle*-shaped cell, formed arrays that appeared to be continuous from cell to cell in the posterior portion of the embryo, but became diffusely distributed in cells within and beyond the bend region (Figure 2-4 B). Concomitant with these changes, the myosin signal in the vicinity of the basal body disappeared (Figure 2-4 E). Post-inversion embryos had very faint myosin signals in the cytoplasm; but a bright spot near the basal bodies reappeared (Figure 2-4 C,

F).

In short, the dynamic changes that occur in myosin II localization during inversion are parallel to those observed for actin filaments, and are as tightly coupled to the morphogenetic events of inversion.

Inhibition of Actomyosin Function Causes Stage-specific Inversion Arrest

To determine what role the observed changes in co-localized actin and myosin might be playing in the inversion process, I examined the effects of four actomyosin inhibitors: cytochalasin B, D, E and BDM (Cramer and Mitchison, 1995). Even when added 2 hours prior to the beginning of inversion, all three kinds of cytochalasin inhibited inversion

Figure 2-4. Localization of myosin II in various stages of inversion.

Each stage is represented by a set of images as in Figure 2-3. Asterisks indicate the embryo coeloms. In a pre-inversion embryo (A,D), myosin was observed in the perinuclear region, and as an intense-labeled spot near each basal body, contractile-vacuole region clearly seen in the magnified image. During inversion (B,E), myosin first became localized in the central, subnuclear regions of the cells, and as in the case of actin filaments, the signal appeared to be continuous from cell to cell (arrowheads), but then as the cells entered and passed the bend region myosin distribution became much more diffuse. Following inversion intense myosin signals reappeared in the basal-body, contractile-vacuole regions of all cells (C,F). Virtually no myosin signal was found at the basal body during inversion (B,E). Bar; 10 μm (A-C), and 5 μm (D-F).
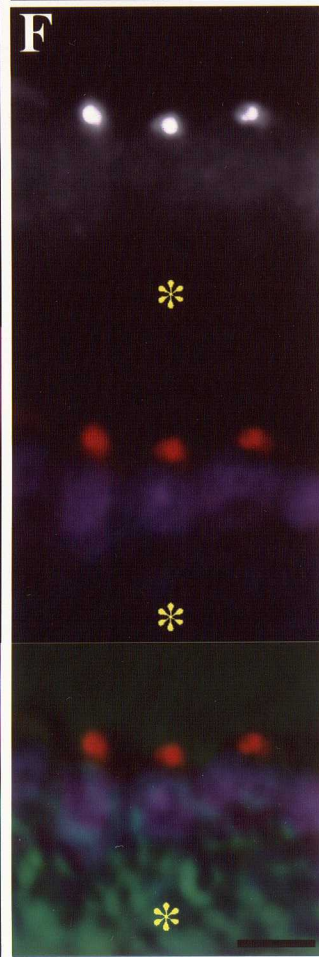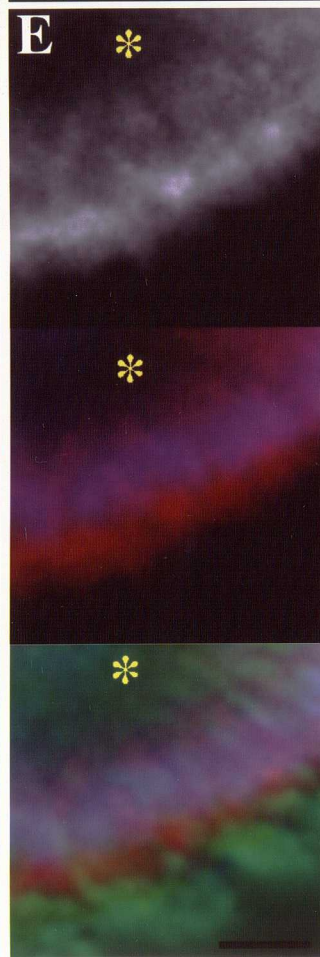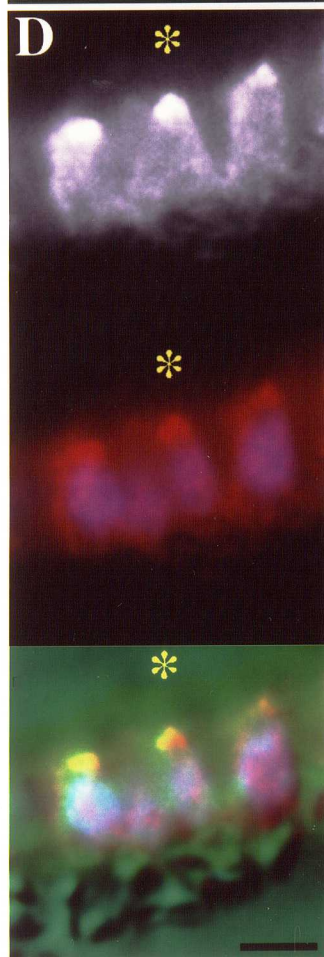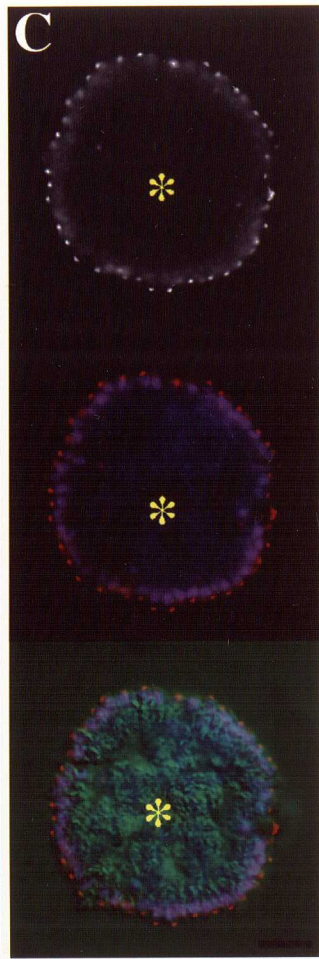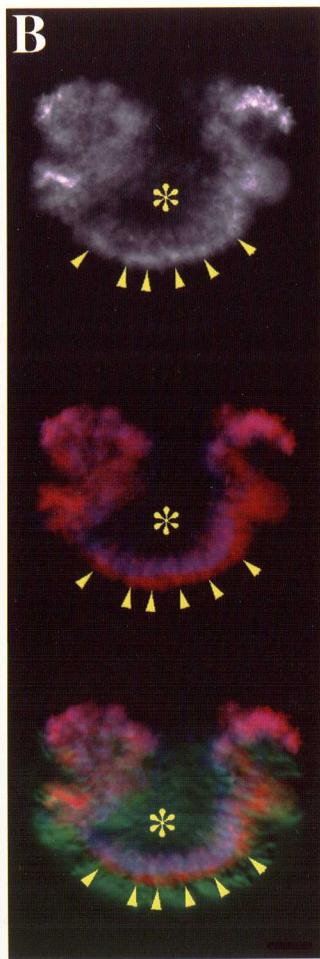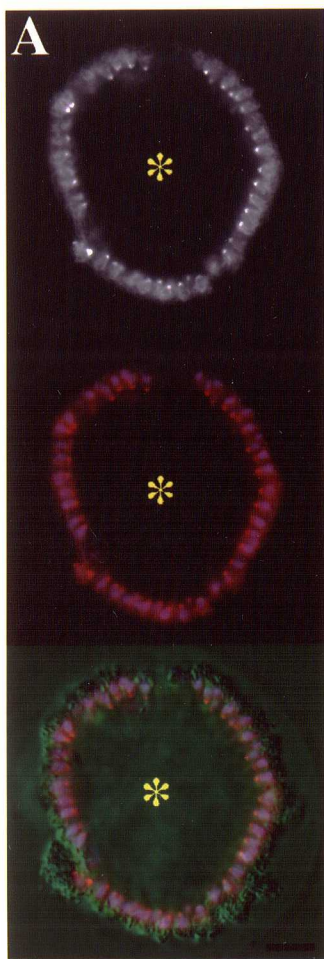
partially (Figure 2-5 F-J), despite the fact that such treatments had led to almost total disappearance of actin filaments in the subnuclear region within the first an hour (Figure 2-6). BDM had the same effect (Figure 2-5 K-O). In all four cases, the phialopore opened (Figure 2-5 F, K) and subsequently the lips of the phialopore began to turn outward (Figure 2-5 G, L), both were similar to that of a control embryo (Figure 2-5 A, B). The propagation of the bend, however, stopped in ~20 minutes, leaving the anterior hemisphere inverted incompletely (Figure 2-5 H-J, M-O). The posterior hemisphere of the treated embryos was never inverted while a control embyro completed inversion (Figure 2-5 E).

In embryos that underwent such an inversion arrest, I noticed that the posterior hemisphere appeared wider than that in control embryos. To quantify this, I measured the diameter of the posterior hemisphere of the treated and untreated embryos, with the results shown in Figure 2-7. In the first 15 minutes after the onset of phialopore opening, the diameter of the posterior hemisphere decreased slowly in both treated and control embryos. But then, whereas the posterior hemisphere of the control embryos decreased in diameter by nearly half during the next 20 minutes, no such rapid decrease in diameter occurred in the treated embryos; they simply continued the initial slow contraction. The time at which abrupt contraction occurred in the control embryos corresponded to the time at which the posterior hemisphere began to pass through the phialopore.

Actomyosin Inhibition Becomes Irreversible Beyond a Certain Time Point

I discovered that BDM acts very rapidly on inverting *Volvox* embryos, and took advantage of this to study the time course of onset and reversal of inhibition more closely (Figure 2-8). When BDM was supplied to an embryo
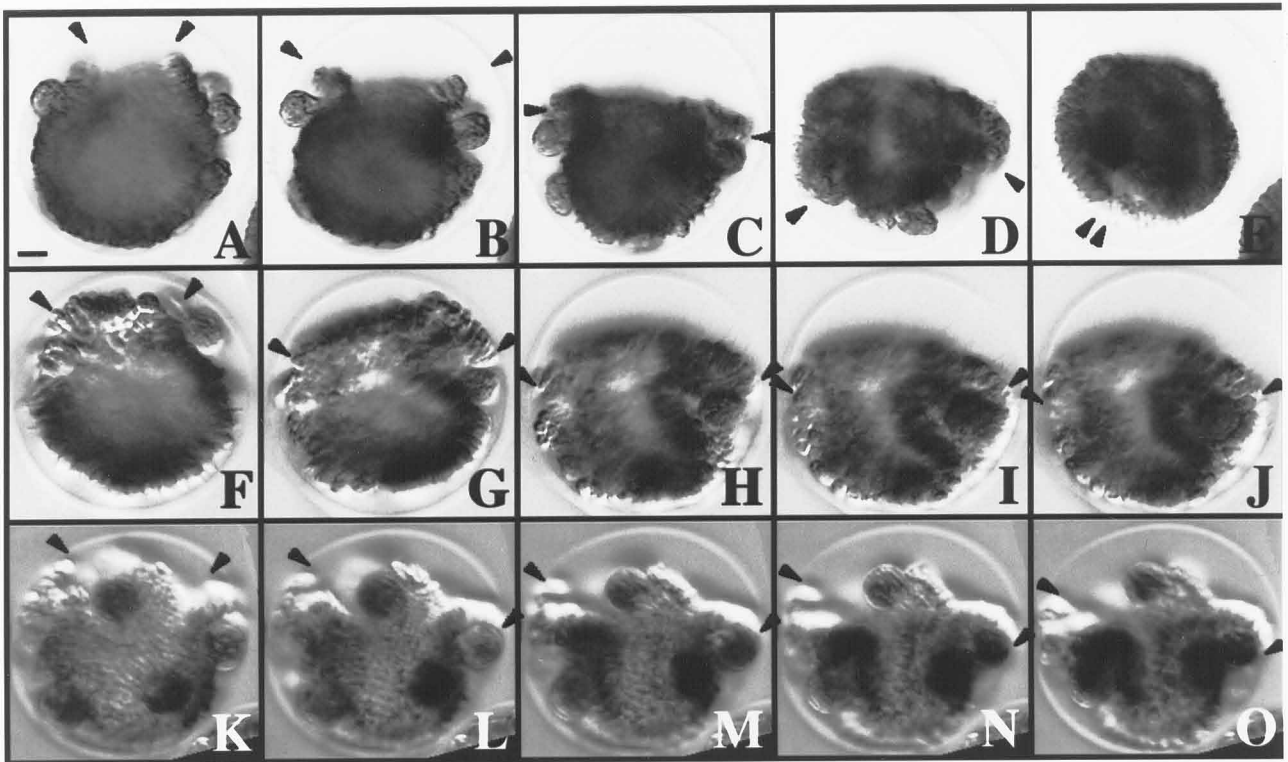
Figure 2-5. Cytochalasin B and BDM cause an arrest of inversion.

Pre-inversion embryos were treated with control buffer only (A-E), 100 μg/ml cytochalasin B (F-J) and 40 mM BDM (K-O) for 2 hours prior to the onset of phialopore opening. Images were captured at 10 minutes intervals after phialopore opening. In the first 20 minutes, the shape of embryos, whether treated or untreated, were similar and the phialopore (arrowheads) opened normally. However, after that time, propagation of the bend was arrested. Bar, 10 μm.
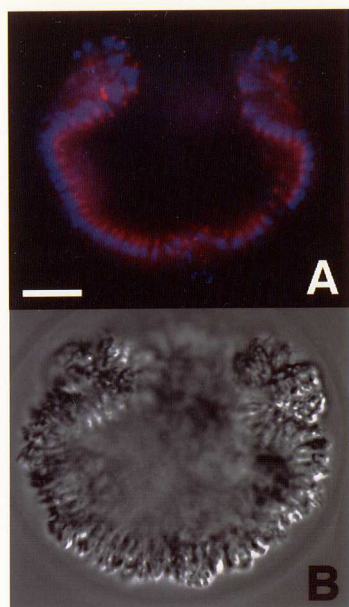
Figure 2-6. Actin filaments that form the inversion-specific belt-like zone were depolymerized with cytochalasin B

With cytochalasin treatment (1 hour), (A, actin filaments in red and the nuclei in blue; B, DIC image) actin filaments were not very abundant, and were restricted to the basal body ends of the cells, whereas in control embryos at this stage actin filaments are very abundant (Fig. 2-3 B, C, F). It is noted that sufficiently long treatment (at least 30 min) is needed to depolymerize actin filaments of *Volvox carteri*. Bar; 10 μm.
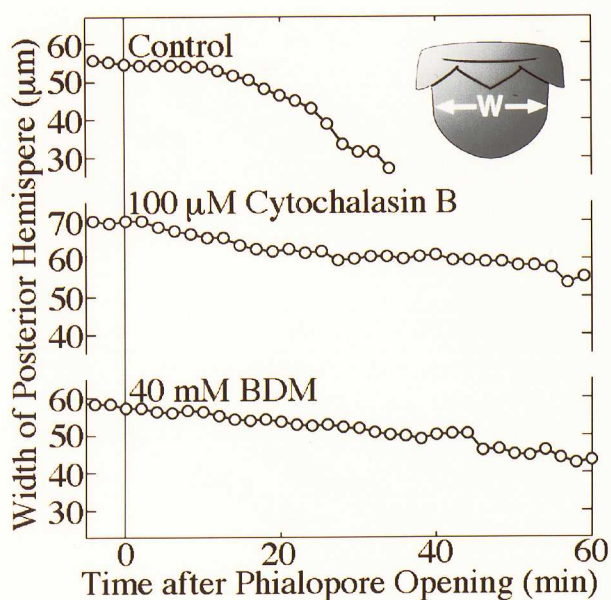
Figure 2-7. Contraction of the posterior hemisphere is inhibited with cytochalasin B and BDM.

The width of the posterior hemisphere indicated as 'w' in the inset picture was measured during inversion. In the control embryo, it decreased gradually in first 15-min, and rapidly after this time point. In the arrested embryos, gradual decrease appeared to be similar to the control but rapid changes never happened. Inversion arrest was found to be accompanied by a failure with shortening of the posterior hemisphere to decrease in diameter.

- 30 -

in which the phialopore had already opened, the posterior hemisphere including the equator expanded significantly within 3 minutes (Figure 2-8 A), obviously which was the inverse progression in inversion of control embryo. Indeed, my measurements (not shown) indicated that the diameter of the embryo at the equator increased by 10-15%. As expected, removal of BDM resulted in a quick contraction that was the converse of the expansion caused by drug exposure (Figure 2-8 B). In this quick expansion and contraction, I could not detect any specific cells or regions that expanded and contracted more than the rest of the posterior hemisphere; the posterior hemisphere appeared to contract almost uniformly. The embryos contracted about 10 μm in diameter, which corresponds to a 15 μm change in the circumference. Taking into consideration that an optical section of the posterior hemisphere shown in Figure 2-5 and Figure 2-8 contained approximately 30 cells, the individual

cells are expected to contract far less than 1 μm. The action of BDM could be fully reversed, even in embryos exposed to the drug for more than 3 hours before phialopore opening, if 'but only if' the BDM was washed out before inversion had been underway for 20 minutes. When the drug was washed out after this time, the treated embryos never completed inversion. This critical time point corresponded roughly with the time at which the abrupt contraction of the posterior hemisphere began in control embryos, as shown in Figure 2-7.

In contrast, the effects of cytochalasins were irreversible in all cases (data not shown). Removal of cytochalasins either before or after the critical time point was unsuccessful. This was probably because of the slow permeation of these chemicals into and out of the embryos.
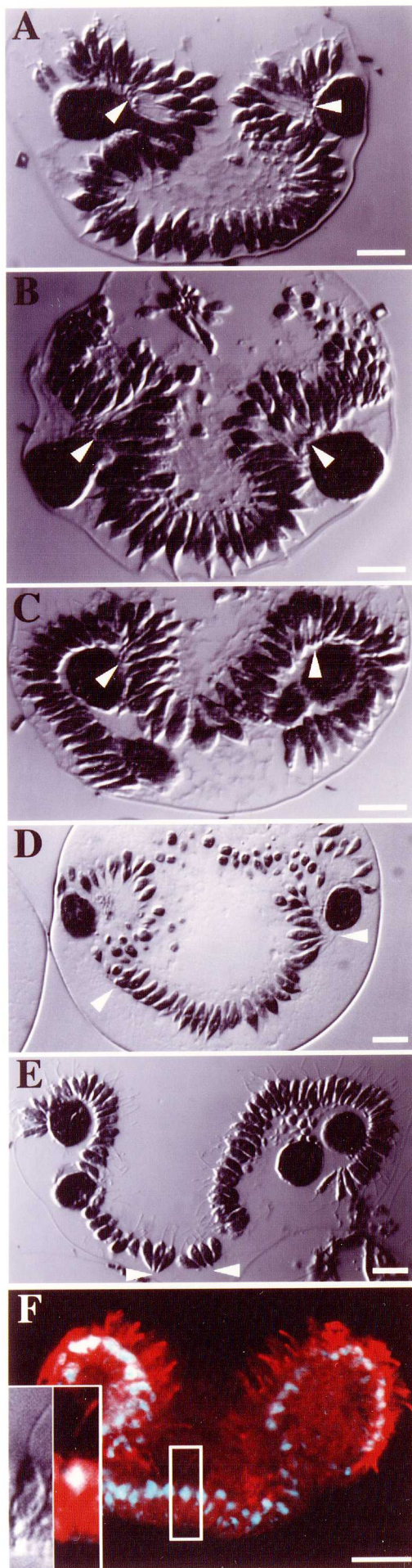
Figure 2-9. Propagation of cell shape changes to the posterior pole in cytochalasin B-treated embryos.

In control embryos, the elongated cells that comprise the bend region were bundled together at the thin ends of the cell (A), and as the bend moved down, this bundling was propagated from the phialopore toward the posterior pole (B-C), as indicated by the arrows. A somewhat similar propagation of cell shape change (arrowheads) occurred in cytochalasin B -treated embryos (D-E). Cells were slightly rounder. the number of cell comprising the bundle was smaller than that of untreated embryos and in some cases the embryo appeared to be fragmented between regions where cells had undergone such apparent bundling. Cytochalasin B-treated embryo had flagella inside the uninverted embryo stained with antibodies to ß-tubulin (red). The nuclei were stained with DAPI (blue). Times after the phialopore opening were; 20 (A), 30 (B), 40 (C), 30 (D), and 50 minutes (E). Bar; 10 μm.

Cell Shape Changes Are Propagated to the Posterior Pole in Arrested Embryos

Results presented in the previous section indicated that a critical point for drug action is passed about 20 minutes after the beginning of inversion, just about the time when the posterior hemisphere of control embryos abruptly becomes smaller and begins to pass through the phialopore opening (Figure 2-5 and 2-7). I speculated that beyond this time BDM and cytochalasins deprive the embryos of the ability to undergo the changes of individual cell shapes that are required to complete the inversion process (Viamontes et al., 1979). However, this speculation was not supported by further examination of cytochalasin B-arrested embryos (Figure 2-9).

In control embryos, as previously reported (Viamontes and Kirk, 1977), a small bundle of extremely elongated *flask* cells (usually about seven cells in a cross section) I was present in each bend region (Figure 2-9 A). This continued to be true as the bend was propagated toward the posterior pole (Figure 2-9 B, C). In cytochalasin B-treated embryos the bend was not propagated beyond the equator to the posterior pole (Figure 2-9 D, E). However, a cluster of elongated cells was not only present in the bend region at the time that inversion was arrested, to my surprise formation of such clusters of elongated cells was propagated beyond the bend within the next 10 minutes (Figure 2-9 D), eventually reaching the vicinity of the posterior pole about 30 minutes after inversion had been arrested (Figure 2-9 E). As in a normal bend region, the thin ends of such cells were bundled together. In the uninverted portion of the inhibited embryo (as in the inverted portion), microtubule staining revealed presence of flagella pointing toward inside the embryo sphere (Figure 2-9 F).
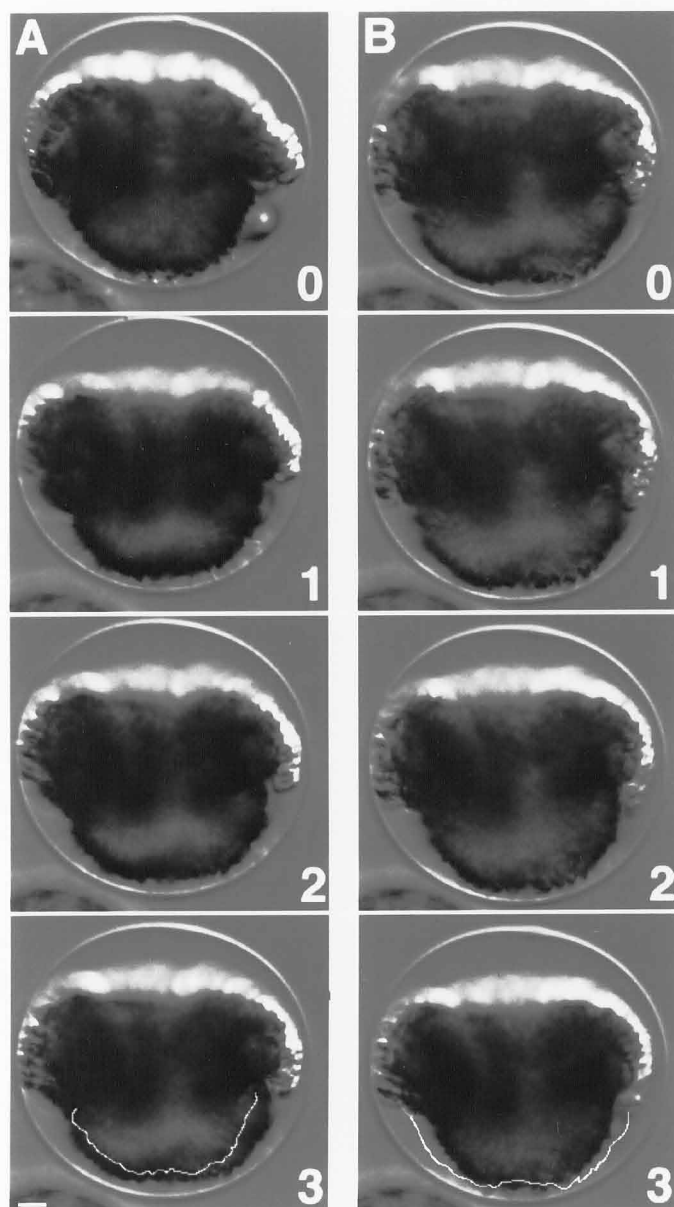
Figure 2-8. BDM relaxes embryos quickly.

(A) Time course of the BDM effect. The phialopore of an embryo had opened, and the bend region was being propagated, at the time when 40 mM BDM was added (top) at time zero the posterior hemisphere became swollen within the next 3 minutes (bottom). The solid line in the bottom panel represents a tracing of the posterior edge of embryo in the top panel added to assist in visualizing the difference that occurred in 3 minutes. (B) Time course of recovery from BDM. After the embryo shown in A had been exposed to BDM for a total of 5 minutes, it was washed with drug-free medium at the new time zero (top). The embryo quickly regained the compact posterior hemisphere. The solid line in the bottom panel represents a tracing of the posterior edge of the embryo at the time the drug was washed out, added to assist in visualizing the extent of the change that occurred in 3 minutes. Bar; 10 μm.

Migration of Cytoplasmic Bridges between Cells Is Not Inhibited in the Arrested Embryos

In principle, it was assumed that the bend of the multicellular sheet in inversion was caused by two cellular processes; (1) cell shape change from *spindle* to *flask* and (2) migration of the cytoplasmic bridges between cells from at the nuclear level to the chloroplast ends. In fact, this well explained the fan-shaped cluster of cells that observed specifically in the bending region. Under the actomyosin inhibitor, however, I observed the same clustered cells that were bundled at their thin, chloroplast ends even in the uninverted posterior hemisphere of the arrested embryos. These unpredictable results suggested that cytoplasmic bridges might be capable of becoming relocated to the chloroplast ends of the cells even in the presence of actomyosin inhibitors. To determine whether this might be the case, the location of cytoplasmic bridges was examined ultrastructurally (Figure 2-10). In BDM-treated embryos (Figure 2-10 A), cells in the posterior hemisphere clearly had cytoplasmic bridges at their chloroplast ends (Figure 2-10 B, C). This embryo had been fixed at a time when inversion would have been completed in the absence of BDM. For comparison, I chose a control embryo with curvature of the posterior hemisphere approximately the same as that of the BDM-arrested embryo, meaning that cells in the posterior hemisphere had not yet experienced inversion at the time of fixation. As previously reported, cytoplasmic bridges were found at the nuclear level (Figure 2-10 D), indicating that bridges in these cells had not yet migrated (Green et al., 1981). In contrast, the cytoplasmic bridges in post-inversion regions (Figure 2-10 E) were located at the chloroplast ends of the cells, like those near the uninverted posterior pole of in the BDM-inhibited embryo(Figure 2-10 B, C). Cytoplasmic bridges migrated similarly in cytochalasin B treated embryos (data
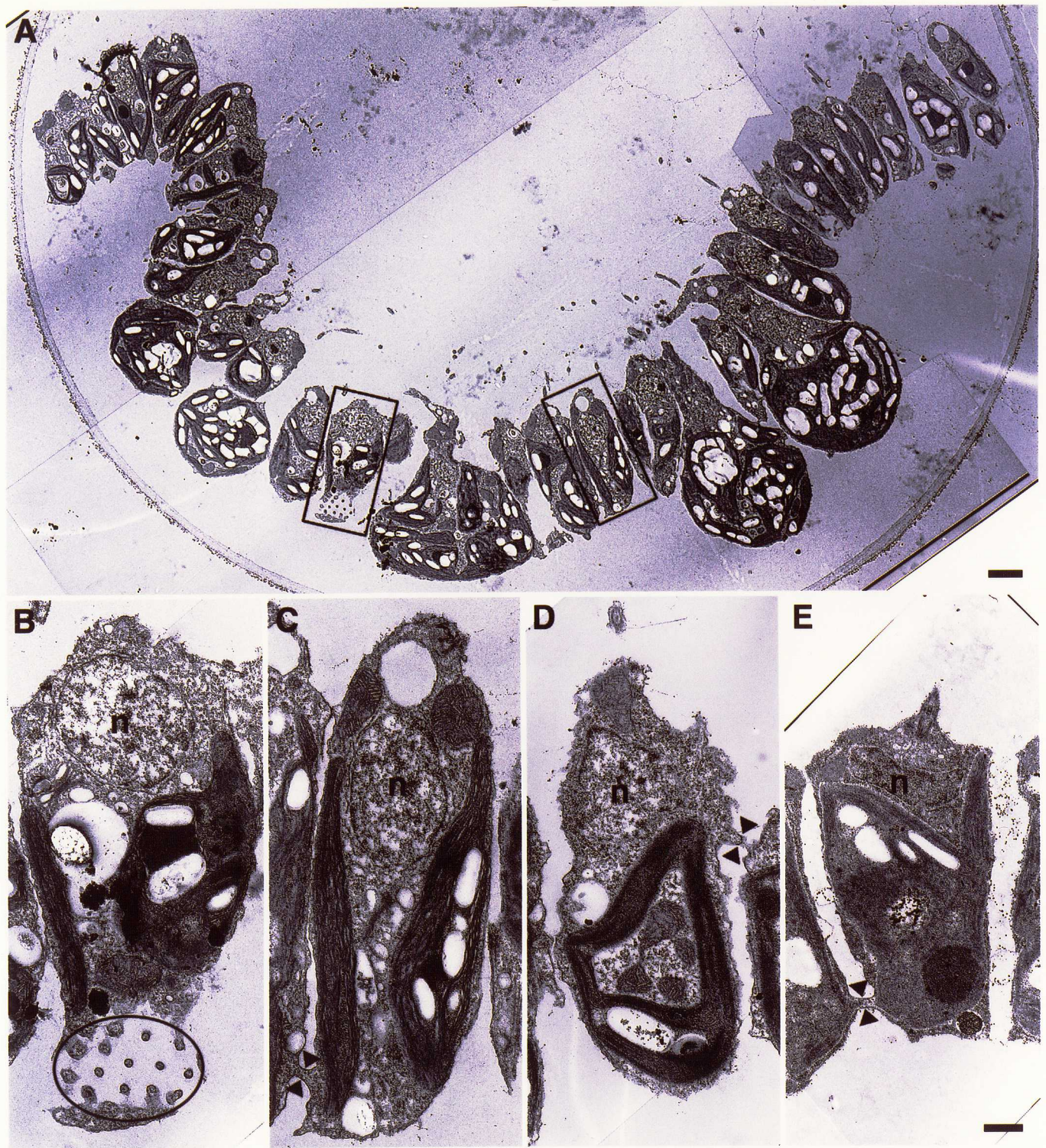
Figure 2-10. Cytoplasmic bridges migrated to the chloroplast ends of cells in BDM-treated embryos.

An arrested embryo was examined ultrastructurally in sagital section (A) to locate the cytoplasmic bridges. The embryos had been treated with 40 mM BDM for 120 minutes prior to fixation. Cytoplasmic bridges of cells near the posterior pole shown in rectangles in A are shown at higher magnification in an en-face section (B; see bridge profiles inside the ellipse) and in a transverse section (C). These bridges are clearly located at the chloroplast ends of cells, far from the nuclear region. An untreated, early-inversion embryo was chosen for comparison that had an overall morphology similar to that of an arrested embryo. In this untreated embryo, cells in locations corresponding to those of B or C had cytoplasmic bridges at the nuclear level (D), and bridges were found close to the chloroplast end only in cells that had entered or passed through the bend region (E). Such repositioning of cytoplasmic bridges in normal inversion was previously analyzed in detail (Green et al., 1981) N; nucleus. Bar; 2 μm (A) and 500 nm (B-E).

not shown). Thus, I needed to hypothesize the role of actin filaments independently from previously assumed two cellular processes.

Inversion Arrest Can be Reversed by Isolation of Embryonic Fragments.

Previously two cellular processes, the cell shape changes from *spindle* to *flask*, and the migration of the cytoplasmic bridges from the nuclei level to the end of chloroplast both took place in the bending region were assumed to well explain inversion (Viamontes et al., 1979, Green et al., 1981). The results obtained above, however, demonstrated that both processes were not sufficient to explain the effect of actomyosin inhibitors that induce the arrest of inversion. If actomyosin inhibitors do not block the propagation of cell shape changes or the migration of cytoplasmic bridges into the posterior hemisphere, why do such inhibitors block inversion of the posterior hemisphere? I postulated that this might be because, in the absence of actomyosin-mediated contraction (Figure 2-7, 8), the diameter of the embryo in the region of the equator is larger than (and hence unable to pass through) the opening that is present in the already-inverted anterior hemisphere.

To test this hypothesis, I performed two kinds of experiment. First, I added BDM to the embryo just after the equatorial region had passed through the bend region. My hypothesis predicted that at this stage BDM would have no effect on inversion at all, because the remaining uninverted portion of the posterior hemisphere would be smaller than the equator. This turned out to be the case (data not shown). The inversion of the posterior hemisphere was not arrested when BDM was added after the equator of the embryo had already passed through the narrow opening.

Second, I used microsurgery techniques to isolate sub-hemispherical fragments of BDM-inhibited embryos (Figure 2-11 A) in which the cut edge

formed an opening as wide as the fragment itself (Figure 2-11). Again, my hypothesis predicted that BDM should have no inhibitory effect on inversion under these conditions. Figure 2-11 shows that this was the case. This also demonstrate the cell shape changes (Figure 2-9) and the migration of the cytoplasmic bridges (Figure 2-10) both appeared to be normally propagated whole embryo in spite of the addition of actomyosin inihibitors had a potential to turn the multicellular sheet outward without the restriction of the narrow opening.
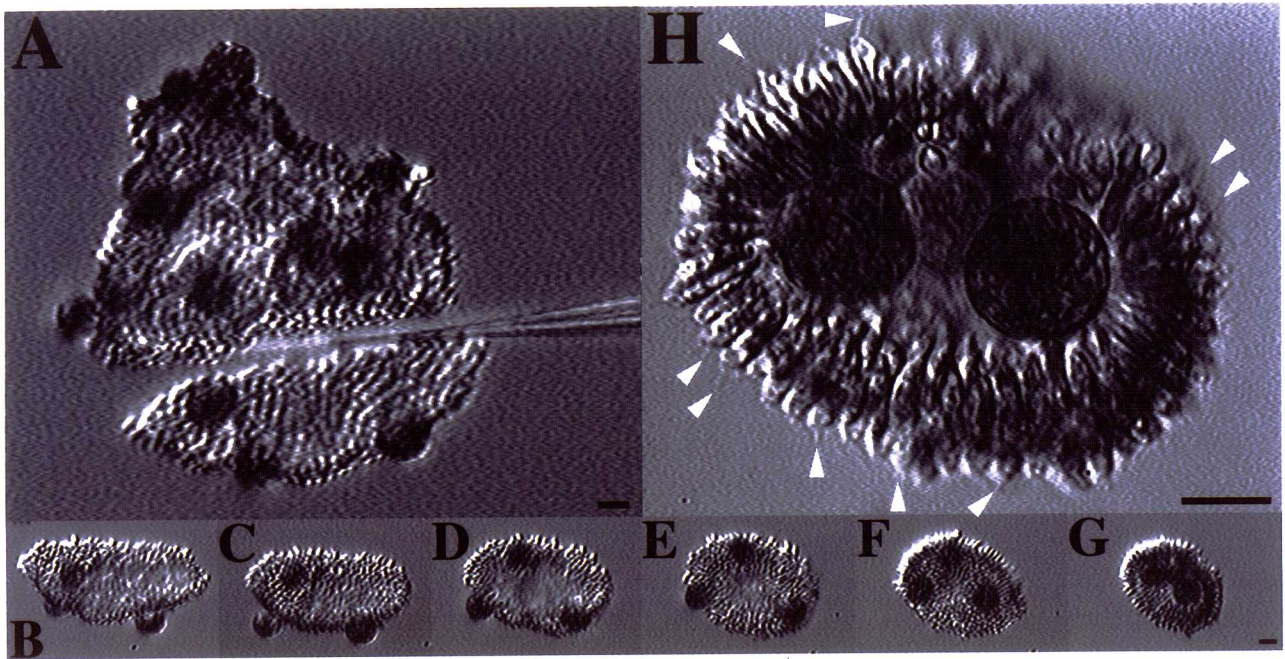
Figure 2-11. Inversion of a posterior fragment can be achieved in the presence of BDM.

A pre-inversion embryo was treated with 40 mM BDM at time zero. With a fine glass needle, it was cut below the equator, closer to the posterior than to the anterior pole; (A). In a side view, three gonidial cells are seen outside the fragments initially (A-C). Between A and H, the dissected posterior fragment rotated about 90° (the initial side view in A became the top view in D) and underwent inversion, so that cells that were initially on the outside (A-C) ended up on the inside (F-H). Flagella (arrowheads) were present on the inverted embryo surface. Time in minutes:seconds after BDM treatment: 12:20 (A), 14:51 (B), 19:50 (C), 22:20 (D), 27:20 (E), 32:20 (F), 37:34 (G) and 37:59 (H). Bars; 10 μm.

Discussion

The immunofluorescence studies performed here indicate that microtubules are present abundantly during the entire course of _Volvox_ inversion, and that changes in their organization correlate with changes in cell shape and embryo morphology. As the clearest example, the long stalks of the flask-shaped cells that are characteristic of the bend region are shown to be richly supplied with aligned microtubules. These observations support the conclusion drawn from ultrastructural observations made by others, that microtubule-mediated changes in cell shape play an important role in the inversion process (Green et al., 1981; Viamontes et al., 1979; Viamontes and Kirk, 1977).

The present study also extends the analysis of _Volvox_ inversion in a new direction by examining for the first time the distribution of myosin and actin filaments in inverting embryos and by

reexamining the effects of actomyosin inhibitors on the inversion process in detail. These studies have uncovered an important aspect of the inversion mechanism that had not previously been detected.

Distribution of Actin and Myosin in Inverting Embryos

As inversion begins, actin and myosin move in concert from the perinuclear region to the subnuclear region of each cell, and then as cells approach the bend region their actomyosin filaments move progressively further from the nuclei, toward the chloroplast ends of the cells. This is reminiscent of the progressive change that has been shown to occur in the locations of the cytoplasmic bridges during the inversion process (Green et al., 1981, Figure 2-8). Moreover, some actin filaments appear to be continuous from cell to cell (Figure 2-3 G). This leads to the obvious suggestion that actomyosin filaments may actually traverse the cytoplasmic bridges that link

neighboring cells (Green et al., 1981). This possibility is certainly worthy of examination at the ultrastructural level, but unfortunately I have not yet succeeded in attempts to preserve the actin filaments of *Volvox* embryos in specimens that are suitable for EM examination (unpublished observation). A similar lack of success has been reported by others (Green et al., 1981; D. L. Kirk, personal communication).

It is particularly noteworthy that the actin-filament network disappears, and myosin becomes diffusely distributed, as soon cells enter the bend region of the inverting embryo (Figures 2-4 C, 2-5 B). This clearly indicates that whatever role(s) the actomyosin complex plays in inversion, that role must be completed before the cells participate in formation of a bend region. This assumption was reinforced by my observation on the effects of actomyosin inhibitors, to be discussed next.

Effects of Actomyosin Inhibitors on Various Aspects of the Inversion Process

All four of the actomyosin inhibitors used here (cytochalasin B, D, and E, plus BDM) had a similar effect when applied to *Volvox* embryos continuously from 2 hours before the beginning of inversion through the time at which control embryos had completed inversion: They permitted inversion to be initiated relatively normally, and to proceed to the halfway of the anterior hemisphere, but they blocked inversion of the posterior hemisphere irreversibly (Figure 2-5).

It was previously reported that cytochalasin D acted on the *Volvox* embryo quickly and reversibly to block both the initial generation of, and the propagation of, the bend regions (Viamontes et al., 1979). Under this treatment, they observed that the migration of the cytoplasmic brideges was inhibited. In contrast, under my conditions of observation all three

cytochalasins acted much more slowly, and irreversibly, and did not prevent either the initial generation of bend regions or their progression in the halfway of the treated embryos (Figure 2-5, 2-6). These slow effects of cytochalasins were taken into consideration in the design in my experiments. I observed with immunofluorescence that no effects on the actin filament network could be observed in the first 5 minutes of cytochalasin treatment (data not shown) and it took 30-60 minutes to fully depolymerize actin filaments in the subnuclear region (Figure 2-6). Thus, cytochalasin treatment for 2 hours before inversion, that I performed here, is thought to be long enough to induce the drug effects in the embryos, and hence the incomplete progression of the bend was never due to insufficient permeation of the drugs. It is unclear whether the different results obtained in this study and the earlier one (Viamontes et al., 1979). These difference between two

studies are due to subtle difference in strains, culture conditions, purity of the drugs, method of drug administration, or some other unknown factor. In any case, the present study and the previous one indicate that the sequence of cell-shape transformations that accompany inversion are largely independent of actomyosin activity, and although they are undoubtedly necessary, they are not sufficient to allow inversion to be completed.

Role of the Force Generated by Actomyosin in Inversion

A clue to the mechanism by which actomyosin inhibitors prevent inversion from going to completion came with the observation that in the presence of such inhibitors the posterior hemisphere of the embryo appeared to be wider than it was in control embryos at the same stage. Measurements confirmed this impression: by 15-20 minutes after the beginning of inversion the posterior hemisphere of control embryos began an

accelerated contraction that reduced its diameter appreciably, but treated embryos underwent no such rapid contraction. The rapidity and irreversibility with which the myosin II inhibitor, BDM (Cramer and Mitchison, 1995) acted on the *Volvox* embryos permitted me to study this phase of the inversion process more closely, and show that an actomyosin inhibitor exerts its inhibitory influence on the inversion process during this period. If BDM was present at the 20-minute time point, inversion of the posterior hemisphere was blocked. In contrast, even in embryos that had been exposed to BDM for 3 hours, if the drug was washed out before the 20-minute time point, inversion was completed normally.

This led me to the hypothesis that actomyosin inhibitors block the last half of inversion by blocking a contraction of the equatorial region of the embryo that is necessary to make it small enough to pass through the opening that is formed by already-inverted anterior hemisphere.

Two additional pieces of evidence supported this hypothesis. The first was the observation that if BDM was added after the equatorial region had passed through this opening, no inhibition of the rest of the inversion process was observed. The second was the observation that if a sub-posterior-hemispherical fragment was isolated by microdissection, BDM failed to prevent it from inverting (Figure 2-11). As shown in Figure 2-9 and Figure 2-10, cell shape changes and migration of cytoplasmic bridges occurred normally even in the arrested embryos. Therefore, removal of the anterior hemisphere, which would otherwise have imposed a physical constraint on the swollen posterior hemisphere, permitted inversion of the arrested posterior hemisphere. In Figure 2-12, I schematize how these mechanics cooperate in inversion with special reference to actomyosin and microtubules. My hypothesis does not require any cellular differentiation between cells in the

- 43 -

anterior and the posterior hemispheres to explain why anti-actomyosin drugs arrest inversion at about the equator.

The role of actomyosin in *Volvox* inversion appears in one sense to resemble the process in which it has previously been shown that actomyosin acts to reduce the dimensions of a multicellular epithelial sheet during animal morphogenesis (Owaribe and Masuda, 1982). It is noteworthy, however, the function of actomyosin contraction may be different in these two cases. Whereas the effect of actomyosin inhibitors in the animal system is attributed to inhibition of the contraction that occurs at one end of each cell and causes them to assume "flask" or "bottle" shape, formation of such cellular shapes in *Volvox* is not prevented by a actomyosin inhibitors, and appears to be driven by microtubules (Figure 2-9; Viamontes et al., 1979). Nevertheless the role proposed here for of actomyosin contraction (namely, to relieve the folding cellular sheet from

the physical constraints) may be applicable in many other examples of epithelial folding, especially when these processes include the passage of a part of the multicellular sheet through a small opening, such as in gastrulation, evagination of imaginal disk (Fristrom, 1988), and so on. Mathematical models of epithelial folding (for example; Odell et al., 1981) might also need to pay more careful attention to resolving such spatial constraints.

I speculate that the disappearance of actin filaments and diffusing myosin both from cells in the already-inverted anterior hemisphere (Figures 2-3 C, 2-4 B) may play an essential positive role in inversion. If the cells were to remain in a contracted state as they entered and passed through the bend regions, this almost certainly would counteract the effect of contractions in the posterior hemisphere, resulting in a decrease in the diameter of the opening through which the posterior hemisphere must pass. Thus loss of actomyosin filaments

and relaxation of cells that have traversed the bend region may well be as indispensable for the completion of inversion as the actomyosin contraction in the posterior hemisphere is.

Mutants called 'Quasi-noninverters' may Include the Strain Lacking the Function of Actomyosin Contraction of the Posterior Hemisphere.

Interestingly, mutants may have the deficiency in the role of actomyosin have been isolated. Sessoms and Huskey (1973), and Kirk et al. (1982) have independently reported mutatns deficeint in inversion, called noninverter and quasi-noninverter. A noninverter was defined as a mutatnt that never initiated inversion and a quasi-noninverter could begin inversion with opening the phialopore but stopped inversion halfway. Especially, Kirk et al. isolated several phenotypes of quasi-noninverters in which the phenotype named 'Tulip' and 'Jester's cap' are special interest because the yound adult morphology of

them looks strikingly comparable with the embryo that arrested inversion with actomyosin inhibitors. As shown in Figure 2-12, I discovered two processes are independent and have different functions both are essential for inversion. From this idea it is a easy prediction that (A) if the microtubule dependent cell shape changes or migration of the cytoplasmic bridges is defient in a mutant, the mutant will show the phenotype that the multicellular sheet will not turn outward and (B) if the actomyosin-dependent contraction of the posterior hemisphere is deficient in another mutant, it will stop the inversion halfway. It seems to be reasonable that at least 2 phenotypes of the mutants, non-inverter and 'Tulip' or 'Jester's cap' were explained well by deficiency in (A) and (B), respectively.

In conclusion, I have shown that actomyosin exerts a contractile force that causes the posterior hemisphere to become compact and thus facilitates the

propagation of the bending region that is generated largely by microtubules. It is undoubtedly necessary for these activities of actomyosin to be coordinated in space and time with the activities of microtubules during inversion. Genetic analysis of these dynamic phenomena may be feasible. A variety of *Volvox* mutants deficient in various phase of inversion have been isolated (Sessoms and Huskey, 1973; Kirk et al., 1982), and techniques suitable for analyzing the molecular basis of such defects have recently been developed (Miller et al., 1993; Schiedlmeier et al., 1994; Hallmann et al., 1997). I am now attempting to isolate transposon-tagged mutants with phenotypes that resemble the drug-arrested embryos of the molecular-genetic program involved in coordinating cytoskeletal activities in space and time to bring about this interesting morphogenetic transformation.
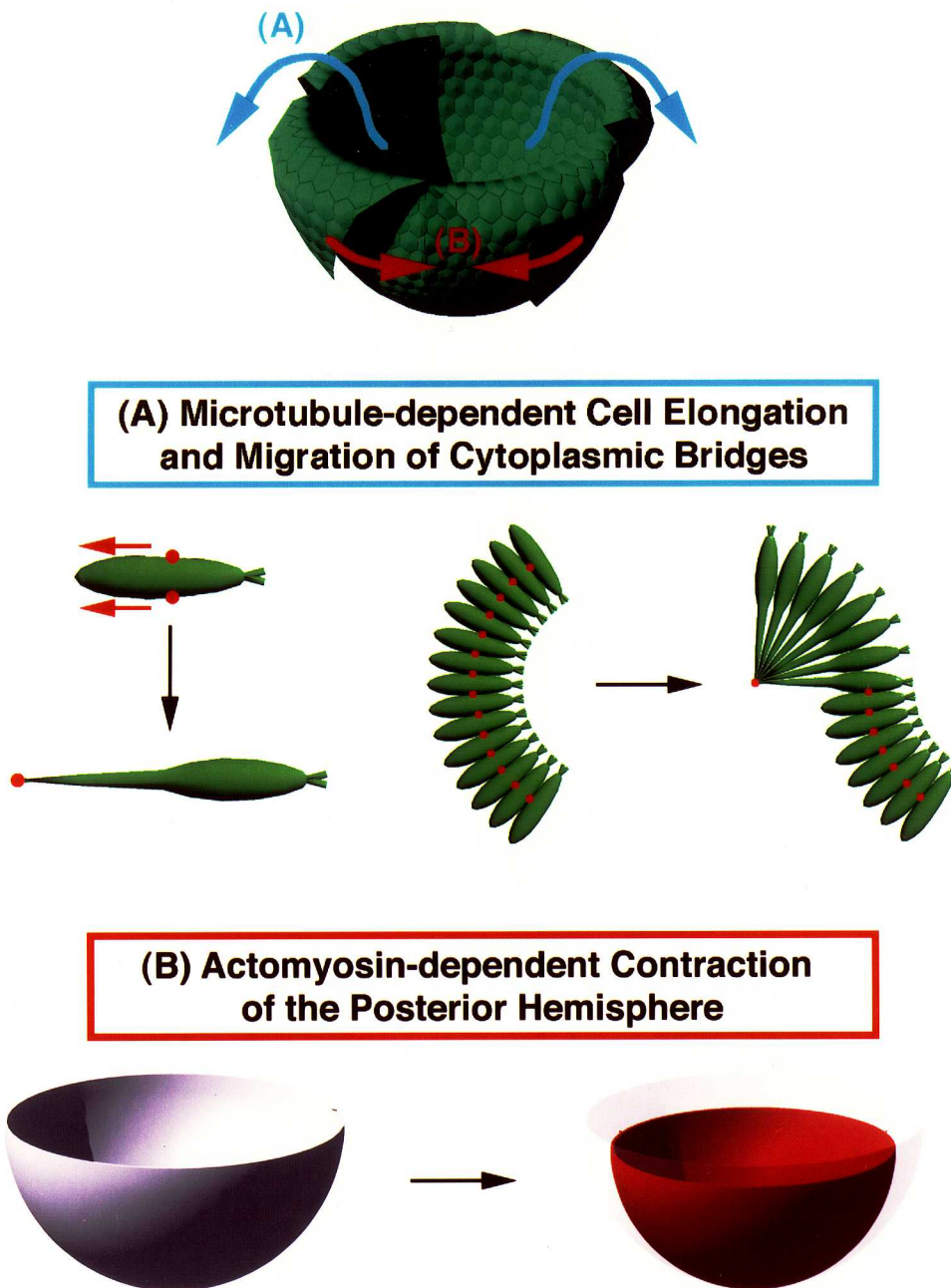
Figure 2-12. Two cytoskeletal components cooperate in inversion of *Volvox* embryo.

Inversion consists of two distinct motions of the multicellular sheet. One starts from the lip opening at the phialopore and the bend propagates toward the opposite pole, making the entire sheet inside out (A). The other is the contraction of the posterior hemisphere (B). Microtubules are responsible for the former process, and actomyosin for the latter. (A) The bend is formed by two different, but both microtubule-dependent changes in the individual cells; the shape changes from spindle to flask cells, and the migration of cytoplasmic bridges. As cytoplasmic bridges (red dots) move away from the basal body, the cell elongates, thus reversing the sheet curvature in the bend. Characteristics of the 'cytoplasmic bridge system' in *Volvox* were studied in detail by Kirk and his colleague (Green et al., 1981). (B) Actomyosin-dependent contraction of the posterior hemisphere makes it small enough to pass through the opening that is formed by already-inverted anterior hemisphere. The 'snap-throw' behavior of the posterior hemisphere, a nomenclature because of the posterior hemisphere inverting faster than the anterior hemisphere, reflects the elastic nature of the multicellular sheet of *Volvox* embryos (Viamontes et al., 1979). We suggest that the molecular mechanism for the 'snap-throw' is likely to be based on the active contraction of actomyosin.

Chapter III
Isolation of Inversion-less Mutants by
Using *Jordan* Transposon-tagged System

Introduction

Mutants Deficient in the Multicellular Sheet Folding Process are Available as Inversion-less Mutants in *Volvox carteri*

Availability of viable mutants in spite of deficient in differentiation is prominent characteristics in *Volvox* as a model organism. More than a quarter of century ago, mutants that have defect in inversion were reported (Sessoms and Huskey, 1973 Figure 5 & 6). Two types of mutant were isolated with chemical mutagenesis. One type was named noninverter of which phialopore never opened and inversion was not initiated. Another mutant was named quasi-noninverter that started inversion but stopped halfway. Concerning quasi-noninverters, several types of pheno-types were reported by Kirk et al. (Kirk

et al., 1982 Figure 3). They were named "Tulip", "Jester's cap", "Mexican hat", and "Bialy", according to the extent of the progression of inversion. Availability of such a variety of mutants in research on multicellular sheet folding has never been reported in any other organisms. Thus, a comprehensive study of inversion-less mutants is expected to result in elucidating a novel aspect of the mechanism of the multicellular sheet folding although it has been long neglected for lack of technology.

Jordan Transposon-tagged System Enables Cloning of Mutants in *Volvox carteri*

Recently, the techniques of the molecular biology in *Volvox* have been progressed rapidly. Remarkably, Miller et al. (1993) established the gene cloning method by using a transposon. The 1,595-bp transposon named *Jordan*

(after a famous basketball player he likes) was cloned by using site of nitA gene that codes nitrate reductase of *Volvox* (Gruber et al., 1992) and shown to possess the unique feature for gene cloning. The gene disruption by random insertion of *Jordan* is possible at enough high frequency. It has been shown that approximately 50 copies of *Jordan* are on one genome and the frequency of the transposition of *Jordan* is increased by heat- or cold-shock treatment. In fact, RegA mutant and GlsA mutant both are deficient in germ-soma differentiation have been isolated by *Jordan* insertion and the both genes are shown to be cloned (Kirk et al. 1999, Miller and Kirk 1999). In addition, the transformation method by particle-bombardment and the gene replacement by homologous recombination have been demonstrated (Schiedlmeier et al., 1994, Hallmann et al., 1997). These techniques have endowed *Volvox* with a new potential. The application of *Jordan*-tagged system to mutants deficient in inversion is indeed attractive. The genetic information of the various mutants is enough valuable since such a mutant that have deficient in the process of multicellular folding has never been isolated in other organisms. In addition, the combination of the molecular genetics with the cell biology techniques is possible *in Volvox* as shown in the previous chapter. For example, the involvement of actomyosin in the quasi-noninverters ("tulip" and "Jester's cap") is intriguing because the phenotypes seem to be similar to the arrested inversion with actomyosin-inhibitors.

It is uncertain, however, that such a mutant can be isolated in the *Jordan*-tagged system. All mutants isolated previously were mutagenized chemically and thus it seems to be caused by point mutation. In contrast, the mutation is insertion in the case of *Jordan*-tagged system. It is very suspicious that the mutants by point mutation are re-produced by insertion. In addition, chemical mutagenesis could be

controlled to produce mutants at high frequency in which condition every spheroid is mutagenized while the frequency of transposition of *Jordan* is unable to accomplish so high. Evidently, the proposal without effective measures to isolate inversion-less mutants is far from reliable.

The screening method that enables the safe isolation of inversion-less mutants is essential. The physiological properties of inversion should be considered. It is not difficult to imagine that the phototaxis is useful for the screening. Apparently the phototaxis of *Volvox* requires the accomplishment of inversion because the flagella, which generate motive force for swimming, normally elongates from the outer surface after completion of inversion. Non-inverter will never swim with no-effective flagella. Even though quasi-noninverters are possible to beat a part of flagella on the surface of the inverted region, their irregular morphology will result in affecting the directional movement. Thus, the selection of less-phototactic mutants is expected to be effective for isolating inversion-less mutants.

In this chapter, I develop the screening method by using phototaxis. It is sufficiently effective and enables me to isolate inversion-less mutants. A part of mutants are re-screened for obtaining revertants and shown to be *Jordan*-tagged by RFLP analysis. The inversion of mutants is also observed and compared with the arrested inversion with actomyosin-inhibitors. This is the beginning for the study of the molecular mechanism of inversion.

Materials and Methods

Parent Strains

Strain CRH22, BCR207, or CMCN8 were used as a parent strain to obtain inversion mutants. These three strains are nitA⁻ which is useful as a marker gene to perform co-transformation experiment to transform a certain interest gene into *Volvox* by bombardment with plasmid-coated gold particles (Schiedlmeier et al., 1994). CRH22 was previously isolated in order to trap *'Jordan'* transposable element within nitA (nitrate reductase-encoding) gene (Gruber et al., 1992, Miller et al., 1993). Thus, this strain was prove to have highly mobile *Jordan* though it is a little unstable since it is possible for this *Jordan* itself to jump out of this site. BCR207 and CMCN8 were mutagenized by drug and selected as nitA⁻ Thus, both strains were stable. Unfortunately, both strains have not been probed to have actively mobile *Jordan* yet even though both were derived from *Jordan*-active strain. All of my mutants below were derived from CRH22, except for Inv001 that was derived from BCR207.

Mutagenesis

Jordan, a classical type of transposon recently found in *Volvox* (Miller et al., 1993), has unique and useful property which is advantage for obtaining and analyzing mutants at the molecular level. It is that the transpositioning rate of *Jordan* is dependent on temperature; when *Volvox* is cultivated at low temperature, i.e. 24°C, *Jordan* jumps at higher frequency than when growing at normal 32 °C.

~10 spheroids of the parent strains in the healthy condition were inoculated into a 500 ml-flask containing 300-ml SVM. It was cultivated at 24 °C for 10-14 days under normal 16L/8D light cycle to accumulate *Jordan* insertion-induced mutants. In my experience, culture for less than 10 days was too sparse and over 14 days a number of spheroids became very small with irregular shape, which was considered to be caused by too dense condition. Thus, 10-14 days culture was compromise between the number of mutants and the size of spheroid for efficient screening.

Screening of inversion-less mutants

The screening of inversion-less mutants were 3 steps; the 1st step was bulky screening in which the spheroids that failed to swim to the light were harvested, the 2nd step was finding the spheroids that looked inversion-failed morphology and in the 3rd step I have confirmed if such morphology was genetic. In the 1st step, I took advantage of the phototaxis of *Volvox*. The embryo that fails inversion naturally lose the ability to swim or to swim in the one direction since the style of swimming of *Volvox* requires a

proper morphology, the spherical shape with flagella outside, which is achieved by completion of inversion. Thus, a spheroid with less-phototaxis is a good candidate for inversion-less. Such spheroids were easy to be harvested in bulk by an apparatus described below.

A flask of 10-14 days-cultivated *Volvox* at 24 °C was used for 1st screening. They were harvested with sterile filter in the light period since phototaxis of *Volvox* was less active in the dark period. Concentrated spheroids were transferred to sterile glass 50-ml syringe and then slowly injected into one end of a glass tube (~60-cm chromatography column with a ~5-cm diameter) that was washed with 70 % ethanol and rinsed with sterile SVM. The glass tube was placed on the flat desk of a clean bench in the dim-light room and in order to induce phototaxis, the opposite end of the tube was locally illuminated with a white fluorescent lamp (5-w). Immediately, some spheroids at the dark end started to swim toward the light end. The population of spheroids contained roughly three groups; fast-swimmers, slow-swimmers and poor-swimmers. The slow-swimmers reached to the goal after 1-3 hours later, and then I discarded the fast- and the slow-swimmers to isolate the poor-swimmers and remaining spheroids were sterilely harvested with filtration. At this step, the poor-swimmers included a relatively large quantity of spheroids although

decreased by 1/50-1/100. When observing them, I could unfortunately see many spheroids with a perfect spherical shape, which were far from my interest. Because they were relatively small and included a relatively small number of somatic cells, the bad growth condition (24°C) was considered to be a part of the reason to produce poor-swimmers. Thus, I transferred them to a new flask with sterile SVM and re-cultivated for 2-3 days at 32 °C to grow them healthfully. They were selected by phototaxis again as above. When still many wild-type looking spheroids were contaminated, the selection was repeated. Usually, screening twice at 32°C was sufficient to isolate mutants in the following step.

In the 2nd step, spheroids selected above were observed under binocular on the clean bench and I picked up spheroids that with abnormal morphology and transferred them to 24-wells plate containing SVM. The criteria I have chosen were a spheroid was enough large and secreted ECM, thus looked adult but (1) gonidia were still outside, (2) a spheroid with opened phialopore. From one flask ≤48 candidates were selected. They were cultivated at 32°C and I selected the strains that inherited their inversion-less phenotype as the 3rd step. More or less 10 strains were usually isolated at this step. If I could isolate more strains, I limited the number less than 10 because the strains from the same clone were considered to be increased.

When the number of spheroids were enough large, I transferred them to bubbling flask to grow in the best condition, and then observed with microscope in detail to finally determine whether the strain was inversion-less or not. Inversion-less strains were stocked in tubes and periodically transferred by Kirk's lab in U.S.A. and by me in Japan.

Culture of Inversion-less Mutants

Inversion-less mutants were cultivated in normal SVM but there were a few things must be cared. First, since the inversion-less mutants that I isolated were considered to be induced by *Jordan* insertion, the contamination of the revertants was easily happened. The revertants always grew better than mutants and thus the careless inoculation may replace the mutant strain with the revertant. The stock culture in 10-ml glass tube that was transferred with one month interval was cultivated at ~30°C to decrease the frequency of *Jordan* transposition. When transferring to a new tube, I always selected the spheroids at the bottom since the spheroids at the top of medium may be revertants.

Second, a few mutants could not survive in the normal culture tube. Especially, Inv001 tended to make large aggregates and I needed to disrupt the aggregations with strong bubbling or suspension by glass pipette. To maintain safely

this strain, flask culture seemed to be the best method. Inv080 also had difficulty to keep healthy. I am keeping this strain in the tube that has a flat bottom.

Screening of Revertants

Revertants are easy to appear when culture at 24°C if the strain is mutated with *Jordan* insertion since *Jordan* jumps again to another site. I had cultivated inversion-less mutant for 7-10 days at 24°C, and then I looked for revertants. The phototaxis was useful at this step, too. It was easy to pick up revertants by placing the flask near the light; the revertants were gathered toward the light but original mutants were still remained. The revertible strain was carefully inoculated to 24-wells plate separately. Stable revertants over 2-3 generations were transferred to flask and cultivated in favorable condition to confirm its morphology.

Preparation of Genomic DNA

For preparation of genomic DNA that is applicable for RFLP analysis, I have used the method (called "mini-prep") previously described (Miller et al., 1993) with modification. Spheroids after 7-10 days culture in 500-ml Erlenmeyer flask were harvested by using 40-μm nylon mesh filter and then washed with excess volume of milli Q water. They were transferred to 15-ml COREX® tube and centrifuged for 10 min at 3000 rpm, with brake-off in order to

suppress the spheroids to float up by deceleration. After discarding supernatant, 200 μl of *Volvox* re-suspension buffer (50 mM Tris-HCl, pH 8; 10 mM EDTA, pH 8) and 300 μl of 10% N-lauroylsarcosine sodium salt (sarcosyl; Nacalai) and 1.5 ml of glass beads (diameter = 400 μm) was added and vortexed at high speed for 1 min 3times with 1 min interval. The tube was then frozen at –80°C and thawed at 37°C five times. After centrifugation at 3000 rpm, the green supernatant was transferred to a clean 15-ml conical tube. An equal volume of 2 x CTAB buffer (2% hexadecyltrimethylammonium bromide (CTAB; Nacalai), 100 mM Tris-HCl, pH 8; 1.4 M NaCl, 1% polyvinylpyrrolidone; Sigma), pre-warmed to 65°C was added, vortexed for 5 seconds, incubated for 5 minutes. The tube was then filled with an equal volume of chloroform, vortexed for 30 seconds and centrifuged for 15 minutes. The aqueous layer was transferred to a new clean conical tube, 1/10 volume of pre-warmed (65°C) 10% CTAB buffer (10% CTAB, 0.7 M NaCl) was added, vortexed for 30 seconds at high speed, incubated for 20 minutes and extracted with chloroform as before. Once again, the aqueous layer was transferred to a new conical tube, and nucleic acids were precipitated with an equal volume of CTAB precipitation buffer (1% CTAB, 50 mM Tris-HCl, pH 8; 10 mM EDTA, pH 8), mixing gently, and allowing to stand at room temperature for 30 minutes. Nucleic acids were pelleted by centrifugation for 10 minutes, the supernatant was discarded, and the pellet was resuspended in 400 μl of high-salt TE (10 mM Tris-HCl, pH 8; 1mM EDTA, pH 8; 1 M NaCl) and the solution was transferred to 1.5 ml Eppendorf tube. Nucleic acids were then precipitated with 1 ml of ethanol at –20°C, pelleted by centrifugation for 10 min, dried, resuspended in 400 μl TE (10 mM Tris-HCl, pH 8; 1mM EDTA, pH 8) and precipitated with 1/10 volume of 3.0 M sodium acetate pH 5.2 and 1 ml ethanol as before. The dry pellet was again resuspended in 300 μl of TE buffer and then 30 μl of 200 mM spermin•4HCl was added in order to precipitate nucleic acids (mix gently). After spinning at high speed for 1 minutes and discarding supernatant, pellet was dissolved in 75 μl of 100 mM EDTA pH 8 and 65 μl of 4.0 M ammonium acetate and incubated over night at 4 °C. Next, 500 μl of 100 mM EDTA pH 8 was added, then suspended vigorously, and stored at 4 °C for 1 hour. Nucleic acids were precipitated with 520 μl of propyl alcohol (Nacalai) at 4°C for 1 hour, pelleted at high speed for 10 minutes, rinsed with 70 % ethanol, and the dry pellet was dissolved in 450 μl of TE buffer, then extracted with an equal volume of phenol, next with phenol/chloroform and finally with chloroform. Nucleic acids were precipitated with sodium acetate and ethanol, and the dry pellet was

dissolved in 200 μl of TE buffer. The yield was typically 20-80 μg.

RFLP analysis

2 μg of gDNA digested with the appropriate restriction endonuclease in the presence of 20 μg/ml RNase A was applied on 0.8% agarose/TAE (40 mM Tris-acetate, 1 mM EDTA) gel (15 x 20 cm) and run at 40 V in circulated TAE. After photographed with a scale bar, the gel was transferred to 0.25 N HCl for 5 min, rinsed with RO-water 5 times, denatured in 0.5 M NaOH and 1.5 M NaCl for 1 hour, rinse again with RO-water, and then 0.5 M Tris-HCl, pH 7.4 and 1.5 M NaCl for 1 hour. DNA in gel was transferred to HyBond-N + (Amersham) by capillarity in 10x SSC (SSC: 0.3 M NaCl, 30 mM sodium citrate) over night. Then, the nylon membrane was rinsed in 5x SSC, dried at 60°C for 30 minutes, and pre-incubated in 10 ml Rapid-hyb buffer (Amersham) for 30 min. For labeling and detection of probes I used Gene Image™ (Amersham) according to the directions of manufacturer, except that following hybridization with the probe, the membrane was washed 4 times with 3x SSC, 0.2% SDS, 5 mM EDTA and 2 times with 0.3x SSC, 0.2% SDS, 5 mM EDTA. ~1.4 kb *Jordan* template was prepared by digestion with Apa I and Nsi I, both unique enzyme sites are located both sides of *Jordan*.

2.7-kb band that showed RFLP of Inv061 gDNA cut with BssH II was sub-cloned as below. 40 μg of Inv061 gDNA was digested with BssH II and electrophoresed on 1.0% low temperature melting agarose at 4°C with circulation. Gel that contained 2.5 kb-3.0 kb DNA were fractionated with razor blade at ~1.5 mm interval. The fractions of gel were melted at 65°C and 1/10 volume of them was examined band by Southern Blot to determine what fraction included 2.7-kb. The remaining gel of *the correct fraction was melted, extracted with* phenol, phenol/chloroform and chloroform, and precipitated with 70 % ethanol. It was ligated at 15°C for 12 hours to pBluescript II KS (-) (Stratagene) that had already been digested with BssH II, purified with gel, and depohosphorylated with CIP (NEB). The ligated DNA was transformed into SURE® cells (Stratagene) with electro-transformation (Gene Pulser® II, Bio Rad). Colonies were transferred to HyBond-N +, treated with 1% SDS for 3 minutes, denatured in 0.5 M NaOH and 1.5 M NaCl for 5 minutes, neutralized in 0.5 M Tris-HCl, pH 7.4 and 1.5 M NaCl for 5 minutes, treated with 2x SSC for 5 minutes and dried at 180°C for 2 hours. Dried membranes rinsed in 2x SSC were treated with 5x SSC, 0.5% SDS, 1 mM EDTA (pH8.0) at 50°C for 30 min and then wiped with Kimwipes. Hybridization and detection were performed as above. The *Jordan*

positive colonies were mini-prepped and their DNAs were digested with BssH II, Hpa I and Hind III to confirm *Jordan* insertion. From one colony, 2.7 kb insertion was produced with BssH II digestion and this has several Hpa I sites and Hind III sites that are characteristics for *Jordan*. This plasmid was sequenced by using BigDye™ terminator cycle sequencing ready reaction kit (Applied Biosystems, Foster City, CA, USA) and ABI PRISM™ 310 (Applied Biosystems). Part of the sequence of 2.7 kb fragment exactly matched to *Jordan* sequence was confirmed.

Microscopy

The photograph of mutants at the young adult stage to compare with wild type was taken by using Olympus SZX12 equipped with Fujix digital camera HC-300/OL system and Macintosh 5500/250. Images were edited with Adobe Photoshop and printed with a color printer (Pictrography 3000).

Video Microscopy

Embryos of mutants were isolated with the method described the previous chapter. They were observed by DIC optics on an Olympus AX-70 and the images were captured with a high resolution cooled CCD camera (PXL-1400; Photometrics) controlled with Macintosh 8600/200 and IPLab.

Results

Screening by Using Phototaxis Effectively Isolated Inversion-less Mutants.

The effective screening method was especially expected when *Jordan* transposon-tagged system was used for isolating inversion-less mutants. Previously reported non-inverters and quasi-noninverters were mutagenized chemically (Sessoms and Huskey, 1973). This means that we could settle the frequency of the mutation by controlling the concentration of a mutagen and thus an optimum condition in which one spheroid had one mutation statistically could be achieved. In contrast, the mutation rate by *Jordan* transposition is dependent on the stress from circumstances such as temperature and unfortunately it is not so high at any condition. It was roughly assumed in a favorable condition (at 24°C) for that one *Jordan* transposon of thousand spheroids jumps to another site per one

generation (S. Miller, personal communication). Even if all 50 copies of *Jordan* on one genome were active, only one of 20 spheroids became mutagenized while remaining 19 were still wild type. Thus, accumulation of more mutants in this condition simultaneously produced much more wild type spheroids in the same flask. In addition, inversion-less mutants had no striking difference from wild-type like some mutants. For example a Reg mutant which is related to germ-soma differentiation (Kirk et al., 1987, Kirk et al., 1991, Tam and Kirk, 1991, Kirk et al., 1999) is colored with denser green than that of wild type and it was easy to be found in a flask even at a glance. Without such easily discernible appearances of inversion-less mutants, too many wild-type spheroids would bury the mutants induced by *Jordan* transposition.

The phototaxis of *Volvox* could be utilized for screening. Noninverters must be immobile because flagella still direct toward the inside of the spheroid as if it

rests oars. Even if quasi-noninverters could move their flagella on partly inverted surface, they might be still less phototactic. The style of swimming that is essential for phototaxis of *Volvox* seemed to require the inversion of the posterior hemisphere because the symmetric and spherical shape with the regularity of anterior-posterior axis has been reported to be essential for phototaxis (Huskey, 1979, Sakeguchi and Iwasa, 1979). In fact, I could confirm that previously isolated strain that possessed the phenotype of quasi-noninverter stocked in Kirk's laboratory could not swim well in the one direction and kept to stay at the same place although it could only spin. These physiological characteristics of inversion-less mutants suggested that an apparatus that would efficiently separate less phototactic spheroids from phototactic wild type would result in selection of good candidates for inversion-less mutants (Figure 3-1 A).

The tube for phototaxis worked well and resulted in selection of less phototactic spheroids (Figure 3-1 B). First, the parent strains, CRH22, BCR207, and CMCN8 were tested. CRH22 and BCR207 were phototactic while CMCN8 wasn't by unknown reason. When I tested remaining two strains after cultivating at 24°C, I noticed that BCR207 partly became less phototactic although most of them were appeared to be still wild type. In contrast, CRH22 was highly phototactic when the screening was performed during the light period (Figure 3-1 B). It is noted that this screening method has no meaning during dark period since *Volvox* doesn't show phototaxis during night. Although screening worked well, when grown at low temperature, the spheroids tended to become too small to identify their morphology clearly under binocular. To avoid this, selected less-phototactic spheroids were transferred to a new SVM containing flask and cultivated at 32°C for 2-3 days in order

to grow healthfully. As a result they have grown sufficiently large and they were selected with the tube again. At this time, the number of the candidates became several thousand and it was possible for me to observe all in ~3 hours. Inversion mutants could be found under binocular, especially quasi-noninverters were easy.

In addition to inversion-less mutants, I could find several types of morphological mutants similar to Reg phenotype, Pcd phenotype (cell division is prematurely ceased in the early cleavage stage), and Cle phenotype (cleavage planes become randomized reported by Kirk et al., 1993). Other unidentified phenotypes were included, too. The irregularity of their morphology appeared to lose the ability of phototaxis.

The phenotypes of inversion-less mutants.

Genetically stable strains of inversion-less mutants were isolated (Table 1) and grown in good condition to examine their morphology. In a few case, there were mutants of which a part of embryos were inversion-less but the remaining ones were wild type and if I isolated and cultivate the inversion-less ones, their progenies were again heterogeneous. Although the mechanism of this phenomenon is interesting, the maintenance of these strains is so hard that I have given them up. Representative phenotypes are described below.

Inv001 was isolated as a typical noninverter, which was only derived from BCR207 in my inversion-less mutants library (Figure 3-2 A). Gonidia continued to stay outside of the embryo while ECM became secreted from soma and spheroid became large as a normal adult spheroid. As a result, this strain had the opposite adult-daughter-granddaughter topology in comparison with wild type (Figure 3-2 B). It is noted that Inv001 was not mobile and tended to form large aggregates so that the
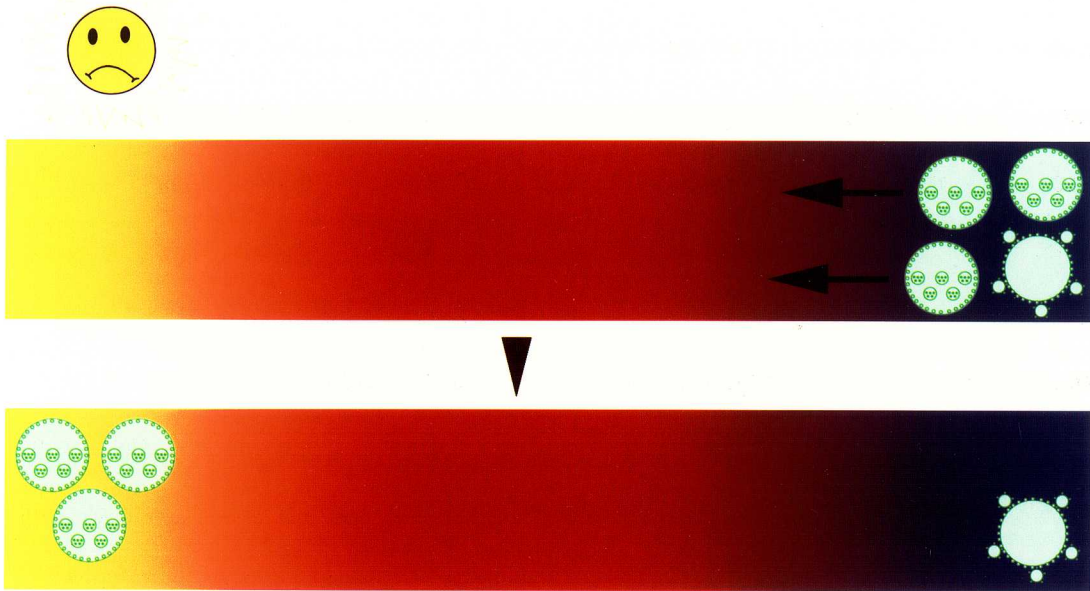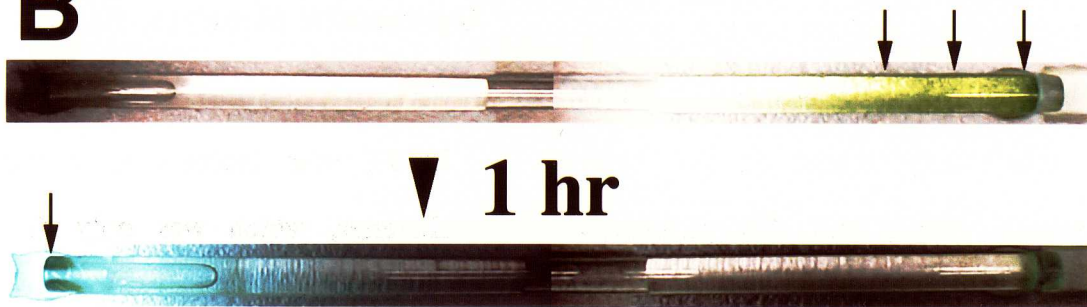
Figure 3-1. Less-phototactic spheroids were selected as candidates for inversion-less mutants.

A. The screening system for less-phototactic spheroids is illustrated. The spheroid that has gonidia outside is a putative inversion-less mutant while other three are wild type. At first they are placed in the right side of the tube. When the opposite side of the tube is lighted up, the phototactic wild-type spheroids are swimming toward the light but the mutant is remaining. This seems to result in selection of inversion-less mutants.

B. A glass tube 60-cm long for chromatography placed horizontally under the sterile hood in the dim light room was used for the screening. Spheroids that were harvested during day-period in the light cycle were injected into the right side of the tube (arrows). When the left side was lighted up and most of the spheroids were reached to the light-end (arrow) in 1 hour. It is noted that this tube did not work when it placed vertically. When it was lighted up from the top, at first spheroids go up but a downward flow that appeared to be caused by the differential density of the spheroids was generated and disturbed the separation.

Table 1, Strains of Inversion-less Mutants

Strain	Type*	Availavility of Revertants
Inv001	G	Yes
Inv014	Q	No
Inv023	Q	Yes
Inv032	Q	Yes**
Inv033	Q	No
Inv034	Q	No
Inv035	Q	Yes
Inv036	Q	No
Inv037	Q	No
Inv038	Q	No
Inv039	Q	Yes
Inv040	Q	No
Inv042	Q	No
Inv044	Q	Yes
Inv046	Q	No
Inv047	Q	No
Inv048	Q	No
Inv049	Q	No
Inv050	Q	Yes
Inv051	Q	No
Inv052	Q	No
Inv053	Q	No
Inv060	Q	Yes
Inv061	Q	Yes***
Inv062	Q	Not dertermined
Inv063	Q	Not dertermined
Inv064	Q	Not dertermined
Inv066	Q	Not dertermined
Inv071	Q	Not dertermined
Inv080	Q	N****
Inv081	Q	N****
Inv082	Q	N****
Inv090	Q	Yes
Inv100	Q	Not dertermined

* Types are classified as G: genuine-noninverter that never starts inversion and Q: quasi-noninverter that initiates inversion but stopps halfway.

** RFLP analysis has shown that genomic DNA of inv032 digested with Aat II has the specific 3.0-kb band probed with *Jordan* while every independent revertants of inv032 loses this band.

*** RFLP analysis has shown that genomic DNA of inv061 digested with BssH II has the specific 2.7-kb band probed with *Jordan* while every independent revertants of inv061 loses this band. This band has already cloned within pBlueScript II.

**** Inv080, Inv081, and Inv082 isolated from the same frask, and all three show the similar phenotype that the phialopore opens but the cell sheet does not fold so much as other quasi-noninverters (see Results). It is highly possible they were from the same clone.
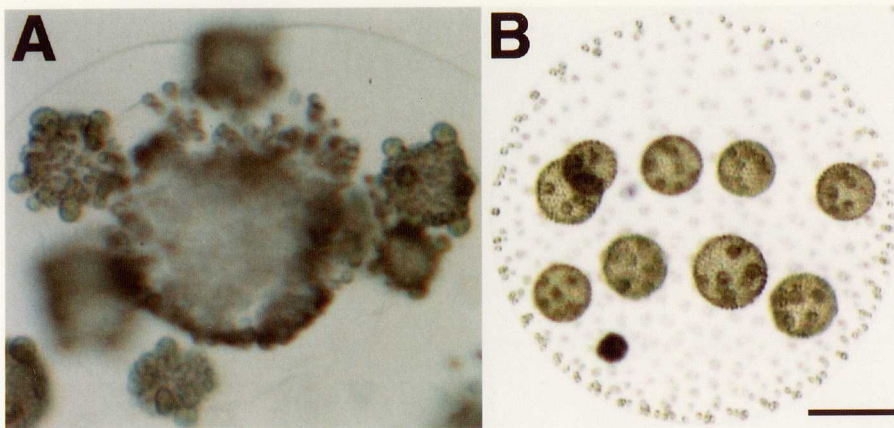
Figure 3-2. Inv001 is a noninverter.

Inv001 (A) isolated from BCR207 is noninverter, which has the opposite topology to wild type (B). Without inversion gonidia continue to stay outside spheroids. Bar, 100 μm.
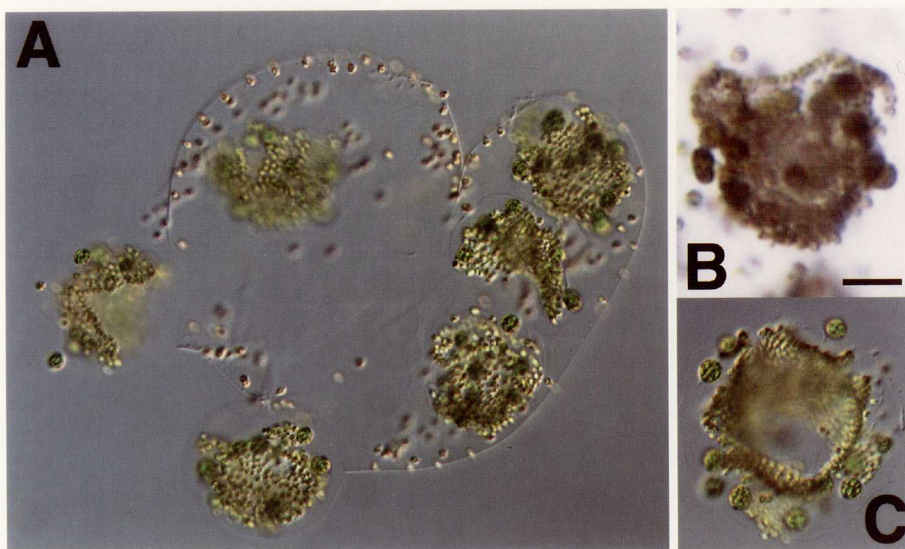

Figure 3-3. Inv080 might have deficiency in cytoplasmic bridges.

Young spheroids of Inv080 show opened phialopore (A) but the cellular sheet appeared not to be curled as other quasi-noninverters (compare B with Figure 3-4 A). In this strain, torn spheroids are often seen (C). This may suggest this strain has a problem in the cytoplasmic bridge system, which connect neighboring cells each other. Bar, 50 μm.
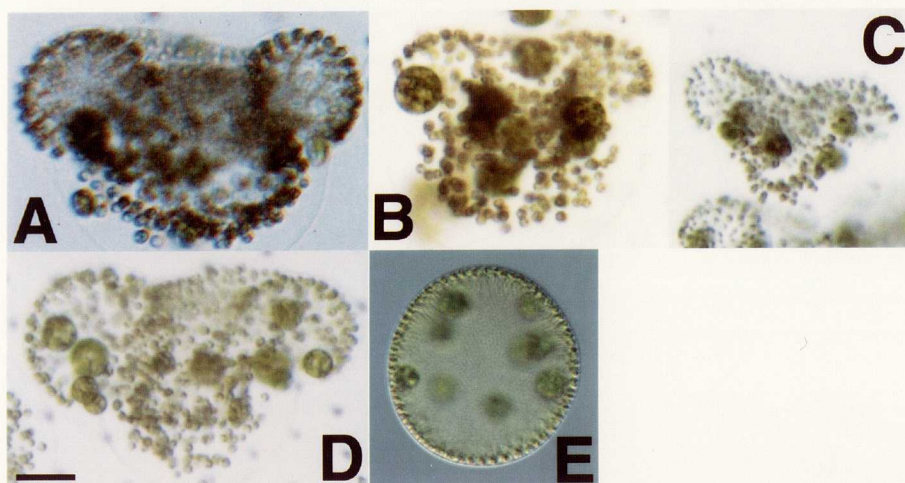

Figure 3-4. Quasi-noninverters

Several quasi-noninverters were isolated A, Inv032. B, Inv061. C, Inv090. D, Inv023. E, reverent of inv061. All strains shown here are revertible, thus I could easily isolated revertants such as E.

agitation for destroying big colonies by strong bubbling or suction by glass pipette was needed to maintain culture.

The rest of the inversion-less mutants were quasi-noninverters of which the phialopore was opened but inversion was arrested halfway. Inv080 has opened phialopore (Figure 3-3 A) and slightly inverted portion (Figure 3-3 B). In comparison with other quasi-noninverters described below, the anterior hemisphere of Inv080 was not so steeply turned outward (compare with Figure 3-4 A, Inv032). When I attempted to observe this strain with video microscopy, it is difficult to find the phialopore. It appeared to begin inversion since the long processes were elongated outward (data not shown). It is rare to see the folding of the cellular sheet. In addition, I often observed torn spheroids of this mutant (Figure 3-3 C). Differently from other quasi-noninverters, this mutants appeared to be incomparable with the arrest by actomyosin inhibitors.

In Figure 3-4, four representative strains of the quasi-noninverters are collected. There were not so large differences in young adult morphology. Inv061 might be less progressed. This difference might be correspond to the difference between "Tulip" and "Jester's cap" but it seems to be difficult for me to distinguish between both. In fact, Inv061 often assumed more progressed morphology and conversely other strains look like Inv061. The individual difference was larger than the difference between these two nomenclature.

Apparently, the phenotypes of them were comparable with the arrested inversion with cytochalasins and BDM as described in the previous chapter. To compare with the arrest by actomyosin inhibitors, they were analyzed with video-microscopy (Figure 3-5). In all three mutants, the inversion was normally started with the opening of the phialopore and then the lips surrounding the phialopore turned outward (Figure 3-5 yellow arrowheads). As inhibited with

actomyosin-inhibitors, inversion was arrested halfway in these mutants. The compaction of the posterior hemisphere appeared to be inhibited, too. The arrest seemed to be similar to that was caused by cytochalasins and BDM.

Two of inversion-less mutants clearly shows RFLP

Revertants were isolated from several strains (Inv001, Inv023, Inv032, Inv035, Inv039, Inv044, Inv050, Inv060, Inv061, and Inv090) by cultivating them at 24°C again for 7-10 days. The isolation of revertants was easy since they recover phototaxis. In the flask revertants go up toward the light, while mutants remained in the bottom so that I just picked up phototactic spheroids from top with a glass pipette. All revertants recovered the spherical morphology. They are perfectly similar to the wild type (Figure 3-4 E).

If revertants are easily isolated from a certain mutant, this is a good evidence that the mutant is caused by transposon.

Especially, *Jordan* is probable since it has relatively higher frequency of transposition at 24°C and moreover, it does not cause frame-shift when it jumped to another site (Miller et al., 1993). In the case of Inv061, it was possible to find a few revertants even 5-days after the inoculation, which contained only several thousand of progenies. It is reasonable by taking account of the transposition frequency of *Jordan* and is hard to explain by a point mutation. In addition, such a high efficiency suggested they were caused by one insertion of transposon. From several mutants (Inv001, Inv023, Inv032, Inv060, Inv061, and Inv090) I could easily isolated revertants while the rate of revertants from Inv035, Inv039, Inv044, Inv050 were low. The highly reverting strains were good candidates for further RFLP analysis.

Inv032 and Inv061 have shown RFLP (Figure 3-6). Genomic DNA of Inv032 digested with Aat II was probed with *Jordan* and a specific band at 3.0-kb was
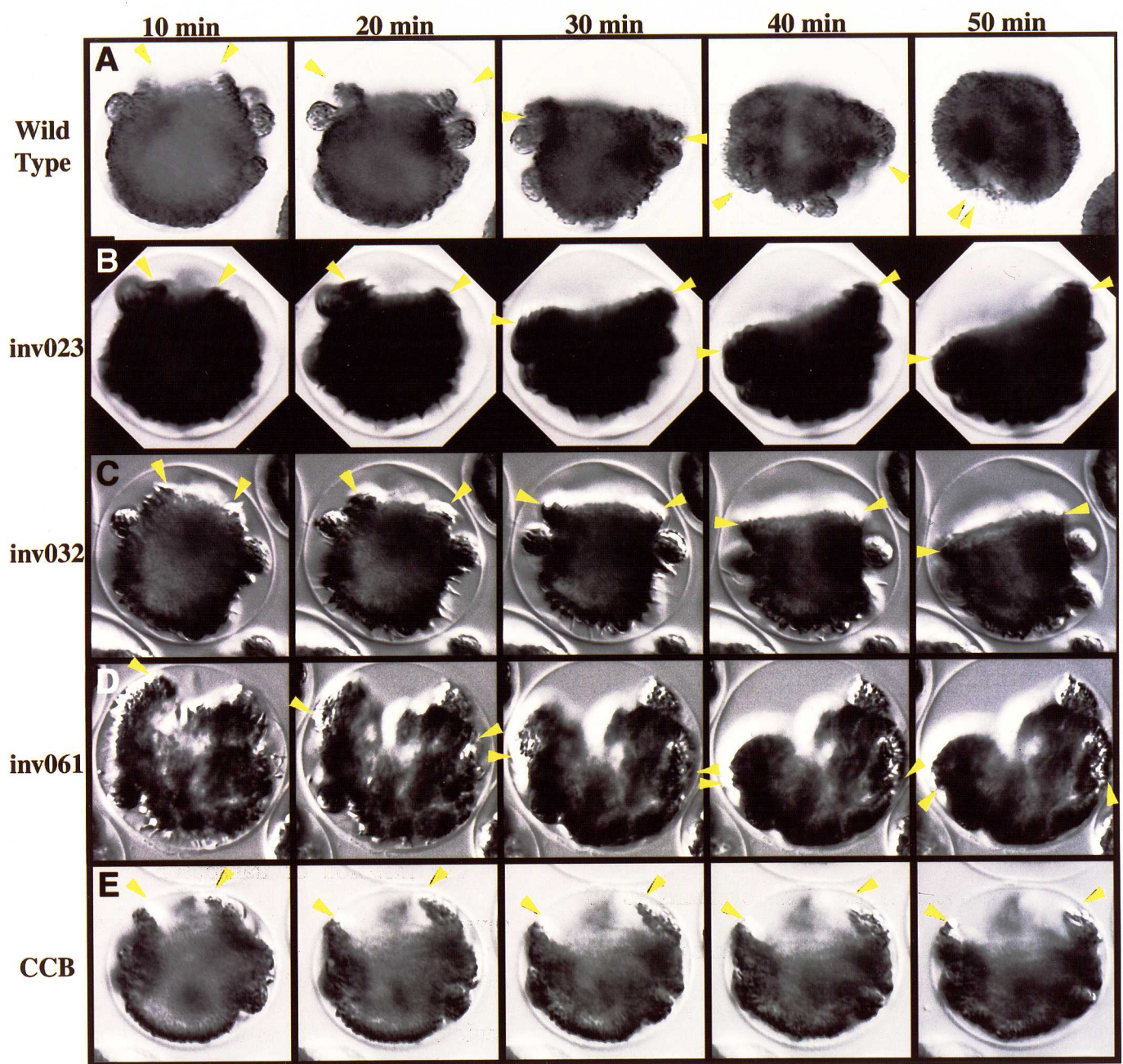
Figure 3-5. Inversion of quasi-noninverters.

The process of inversion in three quasi-noninverters is shown with 10-minute interval. A. Inversion of wild type (same as Figure 2-5) as reference. B: Inv023. C: Inv032 D: Inv061. E: Cytochalasin B-treated embryo (same as Figure 2-5) as reference. The phialopore of each mutant was opened (10-min) and then the lip surrounding the phialopore turned outward progressively as wild type (20-min) as indicated with a pair of arrowheads. The propagation of the bend, however, was arrested before 30-min and never progressed (40- and 50-min). In 10-30 minutes, the processes elongated from the somatic cells in the posterior hemisphere were seen in mutants as same as wild type. This suggests that the microtubule-dependent cell shape changes are occurred in these mutants. Bar, 10 μm.
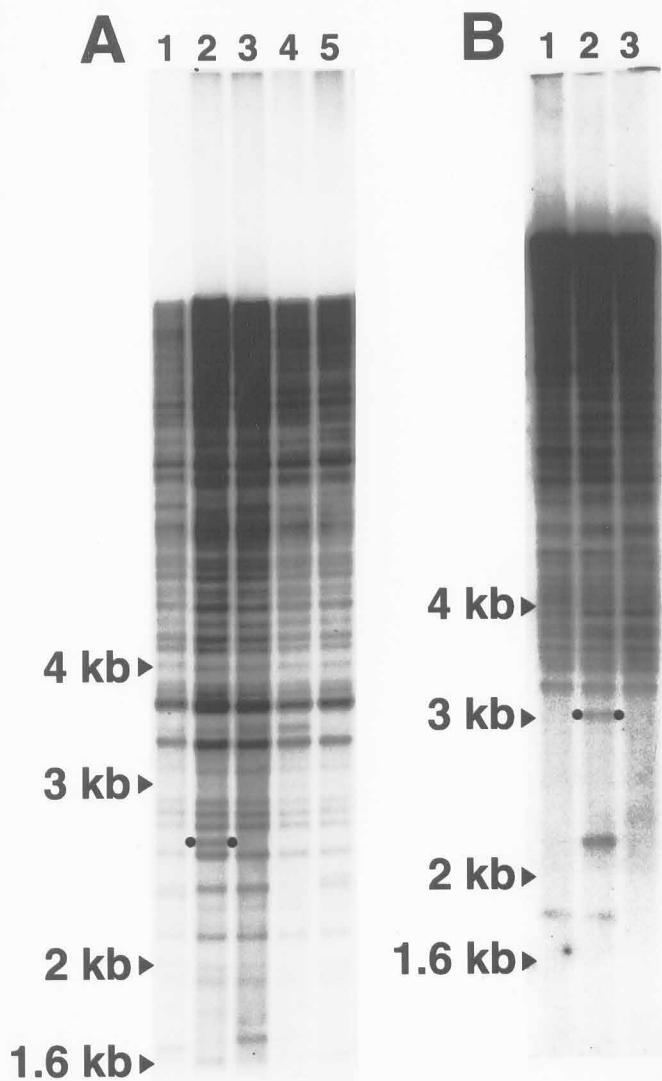
Figure 3-6. RFLP analysis of two quasi-noninverters with *Jordan* probe.

Genomic DNAs were cleaved with an appropriate restriction enzyme, electrophoresed on a 0.8 % agarose gel, and transferred to a nylon membrane; the resulting DNA gel blot was probed with Jordan. A. Genomic DNAs of CRH22 (1), inv061 (2), and independently isolated three revertants (3-5) were digested with BssH II. 2.7-kb band (between dots) of inv061 was specifically probed while CRH22 did not possess it and all revertants re-lost it. B. In the case of inv032, Aat II produced specific 3.0-kb band (between dots). (1) CRH22, (2) inv032, (3) revertant. Although a band around 2.4-kb was specific other revertants still possessed it (not shown).
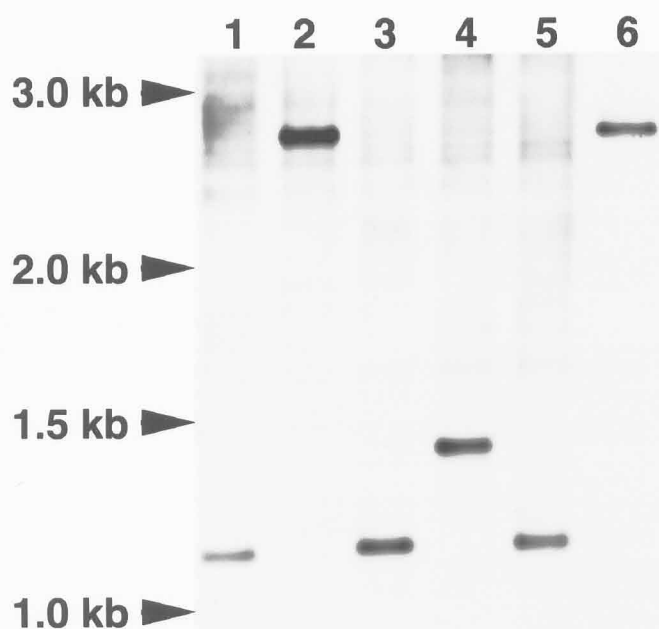
Figure 3-7. Inv061 RFLP fragment is subcloned.

2.7 kb RFLP fragment of Inv061 (Figure 3-6 A) was sub-cloned into pBluescript. Non-Jordan region was used as a probe in this blot. 1, CRH22 (parent strain). 2, Inv061. 3-5, Revertants. 6, Sub-cloned plasmid. The size difference between CRH22 and Inv061 is about 1.6 kb corresponding to the size of *Jordan* transposon. It is noted that one revertant (lane 4) has a larger fragment. This may mean a part of *Jordan* is still remained.

found (Figure 3-6 B). This band was not seen on CRH22 (parent strain) and on several revertants that isolated independently. In the case of Inv061, when digested with BssH II 2.7kb-band shows polymorphism (Figure 3-6 A). Unfortunately, I could not find RFLP for the other mutants though I have used Aat II and BssH II in the addition of more than 10 restriction enzymes. Thus, the other mutants may have the insertion in other. Extensive tests of variety of the restriction enzymes are expected to result in finding RFLP for them.

The 2.7-kb fragment of Inv061 was successfully isolated and ligated to pBluescript although Inv032 have not done yet. In order to remove the region of *Jordan*, 2.7-kb fragment was digested with Hpa I and Hind III and the remaining 1.1-kb fragment was used as a probe for genomic Southern Blot (Figure 3-7). As Expected, 2.7-kb of Inv061 was probed and 1.1-kb band of CRH22 (parent strain) and a part of revertants were probed. The size of 1.1-kb is

reasonable since *Jordan* is 1595-bp (Miller et al., 1993) that corresponds to the size difference between CRH22 and Inv061. Nevertheless, one revertant had a band at 1.4-kb, which was larger than 1.1-kb. This means that a part of *Jordan* was remained when *Jordan* jumped to another site in this revertant. I observed the morphology of this revertant and I could not find any difference from other revertants and wild type. The part of this 2.7-kb fragment was sequenced and it exactly matched to *Jordan* sequence (Miller et al., 1993).

Discussion

Importance of Isolation of Inversion-Less Mutants by *Jordan* Transposon-tagged System

Morphological mutants were readily screened by using physiological characteristics in *Volvox*. Phototaxis, which is a common property of light-dependent organisms, was postulated to be achieved as a result of inversion. The less-phototactic spheroids screened by the method described here were shown to include inversion-less mutants and exclude wild type. This method also enabled selection of other types of morphological mutants. It seems to be a highly potential method for wide-range screening of morphological mutants in *Volvox*, which the relative mutants were never obtained in other organisms.

The efficiency of this screening method well compensated the defect of the low frequent mutagenesis in *Jordan*-tagged system. If the effective screening was not available, I had to select them one by one under the binocular. Apparently, it is a labor to look for mutants in a sea of wild type spheroids and it can not be avoided to miss the morphological mutants that are not so different from wild type. Before I started the screening it was suspicious that inversion-less mutants that used to be isolated by chemical mutagenesis, which meant point mutation, could be re-isolated by *Jordan* insertion. Even under such unsuitable condition, the accomplishment of obtaining several mutants is resulted from the innovation of the screening method. The combination of *Jordan* transposon-tagged system and the phototaxis-screening will be applicable for analysis of other unique morphological mutants of *Volvox*.

Inversion-less mutants isolated here contained not sole but at least three phenotypes. When they are compared with previously reported 6 phenotypes ("Noninverter", "Tulip", "Jester's cap", "Mexican hat", "Bialy", and "Doughnut") three similar phenotypes

are included. Inv001 is noninverter. Most of quasi-noninverters resemble either of "Tulip" and "Jester's cap". More kinds of mutants would be expected to be obtained by performing more screening. A part of those mutants are caused by insertion of transposon since they are frequently reverted (Table 1, Figure 3-4 E). Especially for Inv032 and Inv061, the insertion is shown to be *Jordan* by RFLP (Figure 3-6 and 3-7). These results demonstrated that various morphological mutants are still viable and available by using *Jordan* transposon-tagged system. This promises the analysis of inversion at the molecular level soon.

Correlation between Phenotypes and Cellular Mechanics

Three types of mutants represented by Inv001, Inv080 and Inv061 (also Inv023 and Inv032) seem to reflect well the cellular mechanism of Inversion. As described in previous chapter, three kinds of processes; (1) cell shape changes (2) migration of cytoplasmic bridges and (3) actomyosin dependent contraction of the posterior hemisphere, cause inversion.

Inv001 may relate to the process (1). Cell shape changes are the most basic process for folding of the multicellular sheet and also work in the opening of the phialopore since thinning all cells results in decreasing the area of the multicellular sheet. Without this cell shape change, inversion seems not to start, and thus this process may be related to Inv001 that never initiates inversion. Of course, there are other possibilities such as a certain initiation signal for inversion may be deficient in Inv001.

If cell shape changes are normal but the cytoplasmic bridges do not migrate or migrate prematurely, it seems that the phialopore will open but the folding of the multicellular sheet will be failed. Interestingly, the phenotypes of Inv080 could be explained by the fault of the cytoplasmic bridge migration. Torn

spheroids (Figure 3-3 C) that frequently observed in this strain suggest the cytoplasmic bridges might have structural problems.

The phenotype of Inv061 and other comparable mutants show the opening of the phialopore and the folding of the multicellular sheet in the anterior hemisphere. It is apparently similar to the arrested inversion with cytochalasins and BDM and thus Inv061 and related mutants seems to have deficiency in actomyosin contraction. The sequential images of inversion of the mutants (Figure 3-5) have shown the similarity. The extent of the progression of inversion is comparable, and the processes elongated from the somatic cells are evidence for cell shape changes. Considering these related points together, the working hypothesis that in these mutants the gene that involved in actin cytoskeleton system have been mutagenized is not so strange. Though I have preliminary examined localization patterns of actin filaments of Inv023 and

Inv032, there was no easily discernible difference from wild type. Since the actin gene on genome *Volvox* is only single (Cresnar et al., 1990), the *Jordan* inversion into actin gene is not expected since actin must be the essential gene. The mutation in actin-or myosin-associated proteins, especially required in inversion, might be possible.

Jordan Insertion into an Intron Causes Inv061.

As shown in Figure 3-7, Inv061 was successfully sub-cloned. The size difference between mutants and wild type or revertant was reasonable for insertion of *Jordan* transposon. It, however, one revertant (lane 4) showed a larger band. This seems to be a part of *Jordan*, ~300 bp still remained while the phenotype of this revertant was similar to the other revertants and wild type. These results suggest that *Jordan* inserted into intron in the case of Inv061, as in the case of the recent paper using the same method to clone *glsA* (Miller

and Kirk, 1999). It has shown that *Jordan* was inserted into intron and resulted in skip of the next exon and thus expressed mutagenized *GlsA* protein. In such a case, the expression of the gene was not completely suppressed and incomplete proteins may be expressed. About Inv061, still unidentified, I should consider this possibility for mutation.

In conclusion, I have successfully invented the efficiently screening method of isolating mutants with abnormal morphology. Combined it with the recently developed transposon-tagged system, I have isolated the several inversion-less mutants, including previously isolated but not analysed phenotypes. Those phenotypes seems to be well linked to the hypothesized cellular evnts although unknown mechnaisms are also involved in. A part of mutants were demonstrated transposon-tagged thus they were promising to be cloned. To analyze these mutants with combination of the

techniques of molecular genetics and cell biology will explore novel stuructual and control mechanisms underlying the folding of multicellulas sheets.

References

Agard, D. A., Hiraoka, Y., Shaw, P. and Sedat, J. W. 1989.
"Fluorescence microscopy in three dimensions." In *Methods in Cell Biology* (ed. D. L. Taylor, and Y. Wang), 30: 353-377. Academic Press, San Diego.

Cramer, L.P., and Mitchison, T.J. 1995.
Myosin is involved in postmitotic cell spreading. *J Cell Biol.* 131:179-189.

Cresnar, B., Mages,W., Muller, K. , Salbaum, J.M., and Schmitt, R. 1990.
Structure and expression of a single actin gene in *Volvox carteri. Curr Genet.* 18:337-346.

Ettensohn, C.A. 1985.
Mechanisms of epithelial invagination. *Q Rev Biol.* 60:289-307.

Fristrom, D. 1988.
The cellular basis of epithelial morphogenesis. A review. *Tissue Cell.* 20:645-690.

Green, K.J., and Kirk, D.L. 1981.
Cleavage patterns, cell lineages, and development of a cytoplasmic bridge system in *Volvox* embryos. *J Cell Biol.* 91:743-755.

Green, K.J., Viamontes,G.I., and Kirk, D.L. 1981.
Mechanism of formation, ultrastructure, and function of the cytoplasmic bridge system during morphogenesis in *Volvox. J Cell Biol.* 91:756-769.

Gruber, H., Goetinck, S.D., Kirk, D.L., and Schmitt, R. 1992.
The nitrate reductase-encoding gene of *Volvox carteri*: map location, sequence and induction kinetics. *Gene.* 120:75-83.

Hallmann, A., Rappel, A., and Sumper, M. 1997.
Gene replacement by homologous recombination in the multicellular green alga *Volvox carteri. Proc Natl Acad Sci U S A.* 94:7469-7474.

Harlow, E. and Lane, D. 1988.
Antibodies: A laboratory Manual, Cold Spring Harbor Laboratory.

Huber, O., and Sumper, M. 1994.
Algal-CAMs: isoforms of a cell adhesion

molecule in embryos of the alga *Volvox* with homology to Drosophila fasciclin I. *Embo J.* 13:4212-4222.

Huskey, R.J. 1979.
Mutants affecting vegetative cell orientation in *Volvox carteri. Dev Biol.* 72:236-243.

Ireland, G.W., and Hawkins, S.E. 1980.
A method for studying the effect of inhibitors on the development of the isolated gonidia of *Volvox tertius. Microbios.* 28:185-201.

Kelland, J.L. 1964.
Inversion in *Volvox.* Princeton University, Ph. D. Thesis.

Kelland, J.L. 1977.
Inversion in *Volvox* (Chlorophyceae). *J. Phycol.* 13:373-378.

Kirk, D.L., Baran, G.J., Harper, J.F., Huskey, R.J., Huson, K.S., and Zagris, N. 1987.
Stage-specific hypermutability of the regA locus of *Volvox,* a gene regulating the germ-soma dichotomy. *Cell.* 48:11-24.

Kirk, D.L., Kaufman, M.R., Keeling, R.M., and Stamer, K.A. 1991.
Genetic and cytological control of the asymmetric divisions that pattern the *Volvox* embryo. *Dev Suppl.* 1:67-82.

Kirk, D.L., and Kirk, M.M. 1983.
Protein synthetic patterns during the asexual life cycle of *Volvox carteri. Dev Biol.* 96:493-506.

Kirk, D.L., Viamontes, G.I., Green, K.J., and Bryant, J.L.J. 1982.
Integrated morphogenetic behavior of cell sheets: *Volvox* as a model. In Developmental order: Its origin and regulation. S. S. and P.B. Green, editors. Alan R. Liss, New York. 247-274.

Kirk, M.M., Ransick, A., McRae, S.E., and Kirk, D.L. 1993.
The relationship between cell size and cell fate in *Volvox carteri. J Cell Biol.* 123:191-208.

Kirk, M.M., Stark, K., Miller, S.M., W. Müler, Taillon, B.E., Gruber, H., Schmitt, R., and Kirk, D.L. 1999.
regA, a *Volvox* gene that plays a central role in germ-soma differentiation,

encodes a novel regulatory protein.
Development. 126:639-647.

Lane, M.C., Koehl, M.A., Wilt, F., and Keller, R. 1993.
A role for regulated secretion of apical extracellular matrix during epithelial invagination in the sea urchin.
Development. 117:1049-1060.

Miller, S.M., and Kirk, D.L. 1999.
glsA, a *Volvox* gene required for asymmetric division and germ cell specification, encodes a chaperone-like protein. *Development.* 126:649-658.

Miller, S.M., Schmitt, R., and Kirk, D.L. 1993.
Jordan, an active *Volvox* transposable element similar to higher plant transposons. *Plant Cell.* 5:1125-1138.

Odell, G.M., Oster, G., Alberch, P., and Burnside, B. 1981.
The mechanical basis of morphogenesis. I. Epithelial folding and invagination. *Dev Biol.* 85:446-462.

Ogihara, S., Ikebe, M., Takahashi, K., and Tonomura, Y. 1983.
Requirement of phosphorylation of Physarum myosin heavy chain for thick filament formation, actin activation of Mg^{2+}-ATPase activity, and Ca^{2+}-inhibitory superprecipitation. *J Biochem Tokyo.* 93:205-223.

Owaribe, K., and Masuda, H. 1982.
Isolation and characterization of circumferential microfilament bundles from retinal pigmented epithelial cells. *J Cell Biol.* 95:310-315.

Ransick, A. 1991.
Reproductive cell specification during *Volvox* obversus development. *Dev Biol.* 143:185-198.

Redmond, T., and Zigmond, S.H. 1993.
Distribution of F-actin elongation sites in lysed polymorphonuclear leukocytes parallels the distribution of endogenous F-actin. *Cell Motil Cytoskeleton.* 26:7-18.

Sakeguchi, H., and Iwasa, K. 1979.
Two photophobic responses in *Volvox carteri. Plant Cell Physiol.* 20:909-916.

Schiedlmeier, B., Schmitt, R., Müller, W., Kirk, M.M., Gruber, H., Mages, W., and Kirk, D.L. 1994.

Nuclear transformation of *Volvox carteri*.
Proc Natl Acad Sci U S A. 91:5080-5084.

Sessoms, A.H., and Huskey, R.J. 1973.
Genetic control of development in
Volvox: isolation and characterization of
morphogenetic mutants. *Proc Natl Acad
Sci U S A.* 70:1335-1338.

Tam, L.W., and Kirk, D.L. 1991.
The program for cellular differentiation in
Volvox carteri as revealed by molecular
analysis of development in a
gonidialess/somatic regenerator mutant.
Development. 112:571-580.

**Viamontes, G.I., Fochtmann, L.J., and
Kirk, D.L.** 1979.
Morphogenesis in *Volvox*: analysis of
critical variables. *Cell.* 17:537-550.

Viamontes, G.I., and Kirk, D.L. 1977.
Cell shape changes and the mechanism of
inversion in *Volvox. J Cell Biol.* 75:719-
730.

Wenzl, S., and Sumper, M. 1986.
A novel glycosphingolipid that may
participate in embryo inversion in *Volvox
carteri. Cell.* 46:633-639.